ESTABLISHING CONSERVATION UNITS AND POPULATION GENETIC PARAMETERS OF FISHES OF GREATEST CONSERVATION NEED DISTRIBUTED IN SOUTHEAST MINNESOTA.

FINAL REPORT FOR THE STATE WILDLIFE GRANTS PROGRAM,
DIVISION OF ECOLOGICAL RESOURCES,
MINNESOTA DEPARTMENT OF NATURAL RESOURCES

Peter B. Berendzen
Department of Biology
University of Northern Iowa
Cedar Falls, Iowa 50614
Phone: (319) 273-7026
E-mail: peter.berendzen@uni.edu

Jason F. Dugan
Graduate Program
Department of Biology
University of Northern Iowa

Jeremiah J. Feltz
Undergraduate Program
Department of Biology
University of Northern Iowa

March 2008

ABSTRACT

Southeastern Minnesota is a distinct geographical region that was bypassed by the last glacial maximum and represents a regional hotspot for biodiversity within the state. Several unique areas characterize the topography of southeastern Minnesota; driftless zone, Paleozoic Plateau, and Iowan Surface. The rivers that dissect this region (Cannon, Zumbro, Root, Upper Iowa and Cedar rivers) are all tributaries of the upper Mississippi River and contain a diverse aquatic flora and fauna. Three North American minnows in the family Cyprinidae, *Clinostomus elongatus* (redside dace), *Lythrurus umbratilis* (redfin shiner), and *Notropis nubilus* (Ozark minnow), have restricted distributions in the drainages of southeastern Minnesota and have been identified as Species in Greatest Conservation Need in Minnesota's Comprehensive Wildlife Conservation Strategy. We examined genetic variation within each species, both mitochondrial DNA cytochrome *b* (cyt*b*) gene sequence and microsatellite data, to identify evolutionary units for directing preservation of the genetic diversity within each species. The results revealed different patterns and scales of genetic variation for each species within southeastern Minnesota. Within *C. elongatus* there was very little cyt*b* variation; however, the microsatellite data revealed significant genetic differentiation by drainage. We recommend that conservation efforts directed towards maintaining the genetic diversity of the redside dace focus on each drainage in which they occur in southeastern Minnesota. *Lythrurus umbratilis* exhibits widespread cyt*b* variation across the range of the species. Within *N. nubilus* there are regional differences in the cyt*b* and microsatellite variation. The cyt*b* data revealed a relationship between the upper Mississippi River Basin and the northern Ozarks and the microsatellite data revealed a separation between populations east and west of the Mississippi River in the upper Mississippi River Basin. We recommend that conservation efforts directed towards maintaining the genetic diversity of the redfin shiner and Ozark minnow focus on the entire region they are distributed in southeastern Minnesota.

INTRODUCTION

Southeastern Minnesota is a unique geographical region that was bypassed by the last glacial maximum, the Wisconsinan approximately 21,000 BP (Culter 2001). In doing so it left very distinct geographical formations intact resulting in an area with a distinct topography. The rivers that pass through this area (Cannon, Zumbro, Root, Upper Iowa and Cedar rivers) are all tributaries of the upper Mississippi River and contain a diverse aquatic flora and fauna. Several unique areas characterize the topography of southeastern Minnesota: driftless zone, Paleozoic Plateau, and Iowan Surface (Fig. 1).

Traditionally, the term driftless has been used to describe this entire region suggesting that it had never been encroached upon by glaciation. However, the "true" driftless zone is confined to a small region of southwestern Wisconsin where glacial remnants have never been found. In fact, the existence of a truly driftless area remains controversial (J. Walters, pers. comm.).

The Paleozoic Plateau lies to the west of the driftless zone and extends from southeastern Minnesota to southwestern Wisconsin, northeastern Iowa and northwestern Illinois (Fig.1). This area is distinguished by steep bluffs and deeply dissected valleys, with clear, cool, high gradient streams (Burr and Page 1986). The Paleozoic Plateau is a relic that was not covered by the Wisconsinan ice sheet, but contains some pre-Illinoian glacial till. However, it appears that glaciers did not dictate the entire landscape of this region, as seen in most other parts of southern Minnesota. It is a bedrock controlled landscape, resulting in the main features derived from bedrock that was laid down during the Devonian, Silurian, Ordovician, and Cambrian periods. Each section of the bedrock has a different hardness and resistance to erosion. Some of this bedrock results in areas of karst topography, which is a landscape shaped by water flowing over and through porous bedrock creating features such as sinkholes, valley streams, springs, and caverns. Devonian carbonate bedrock, usually limestone or dolomite, is a source material for karst topography. These factors worked together to create formations controlled by the surrounding bedrock rather that the effects of past glacial episodes. However, there is evidence of some glaciation in this region. The valleys contain pockets of glacial till, which are represented as thin, erosional remnants in the uplands filling some bedrock valleys (Hobbs, 1999).

The Iowan Surface is on the western border of the Paleozoic Plateau in northeastern Iowa and southeastern Minnesota (Fig. 1). This region is thought to reflect a post-glacial topography that developed on 15 – 30 meters of glacial till that was deposited by pre-Illinoian ice sheets (Ruhe et al. 1968; Iqbal 1998). It is in this till that the Cannon, Zumbro and Root rivers of southeastern Minnesota dissected deep valleys and fast flowing streams on their path to the Paleozoic Plateau. The streams eroded out valleys and created a rolling landscape that is devoid of the bedrock formations found to the

east; although some lower karst features, such as sinkholes, remain. The Iowan Surface differs drastically from the Paleozoic Plateau; the area is not bedrock controlled, and prominent bedrock features that might have been there were ground down, scattered and deposited as small pieces of pre-Illinoian till.

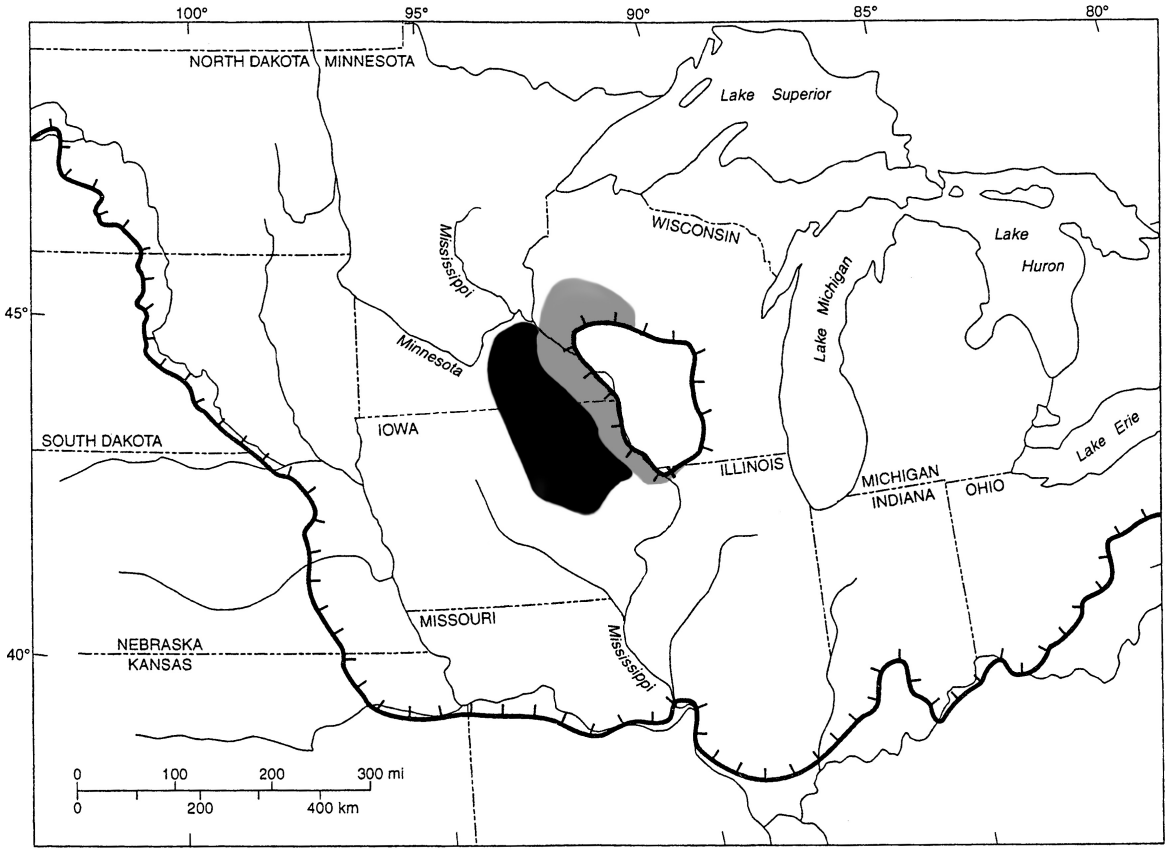

Figure 1. Map of the upper Mississippi River Basin modified from Hobbs (1999). Dark line represents estimated pre-Illinoian maximum limit of glacial expansion, open area in southeastern Wisconsin represents estimated driftless zone, light shaded area represents estimated Paleozoic Plateau and dark shaded area represents estimated Iowan Surface.

This unique portion of the upper Mississippi River Basin has been recognized as a refugium for a number of different organisms during glacial episodes throughout the Pleistocene; e.g. blue-spotted salamander, *Ambystoma laterale* (Demastes et al. 2007) and eastern chipmunk, *Tamias striatus* (Rowe et al. 2004). Following glacial retreat, organisms surviving in this refugium expanded their ranges. This region has also been recognized as containing a unique diversity of organisms that are in need of protection. In 1989, the Driftless Area National Wildlife Refuge in northeastern Iowa was established to help to recover two federally listed species: the endangered Iowa Pleistocene snail, *Discus macclintocki*, and the threatened plant, Northern monkshood, *Aconitum noveboracense*.

Southeastern Minnesota represents a regional hotspot for biodiversity within the state. Therefore this region is a focus of conservation efforts to help maintain the species composition of Minnesota's native fauna. Many of the fishes that occur in the region have restricted distributions and have been identified as in need of conservation. Three North American minnows in the family Cyprinidae, *Clinostomus elongatus* (redside dace), *Lythrurus umbratilis* (redfin shiner), and *Notropis nubilus* (Ozark minnow), are distributed in southeastern Minnesota and have been identified as Species in Greatest Conservation Need (SGCN) in Minnesota's Comprehensive Wildlife Conservation Strategy (CWCS). These fishes are of particular importance and concern because they exhibit a replicated pattern across their entire range (Mayden 1988). Their distributions include portions of the upper Mississippi River Basin, Ozark Highlands in Missouri and Arkansas, Appalachian Mountains of eastern North America, and previously glaciated regions of the Ohio River and Great Lakes drainages. The occurrence of these fishes in tributaries of the upper Mississippi River Basin is thought to be the result of relict populations from Pleistocene glaciations (Burr and Page 1986).

Clinostomus elongatus (redside dace) is a small minnow reaching a maximum length of 8 cm and is characterized by a thin, laterally compressed body and a very large terminal mouth with the lower jaw projecting beyond the upper (Becker 1983). In life their back is blue or blue-green in color and an orange or red streak extends on the sides from the opercle to the origin of the dorsal fin (Fig. 2). The redside dace is contained in the genus *Clinostomus*, which consists of only two species, *C. elongatus* and *C. funduloides* distributed in eastern North America.

Figure 2. *Clinostomus elongatus* (redside dace) collected from the Zumbro River Drainage, Goodhue Co., MN. Photo by the Fish Genetics Laboratory, University of Northern Iowa.

The redside dace is found in slower moving portions of small, cool, silt-free headwater streams with exchanging riffle-pool geomorphology and overhanging vegetation (Becker 1983; Novinger and Coon 2000). They tend to favor mid-water locations in the deepest portions of pools (Novinger and Coon 2000). *Clinostomus elongatus* spawns in the spring in the slow moving riffles adjacent to pools. They typically spawn in the depression behind creek chub (*Semotilus atromaculatus*) or similar species' nests (Becker 1983). The redside dace reaches sexual maturity in 2 – 3 years and can live for up to four years. Their diet consists of both terrestrial and aquatic invertebrates and they are often seen jumping out of the water to capture aerial insects. Feeding success is thought to decrease as the turbidity of the water increases, because the redside dace is a visual predator (Novinger and Coon 2000).

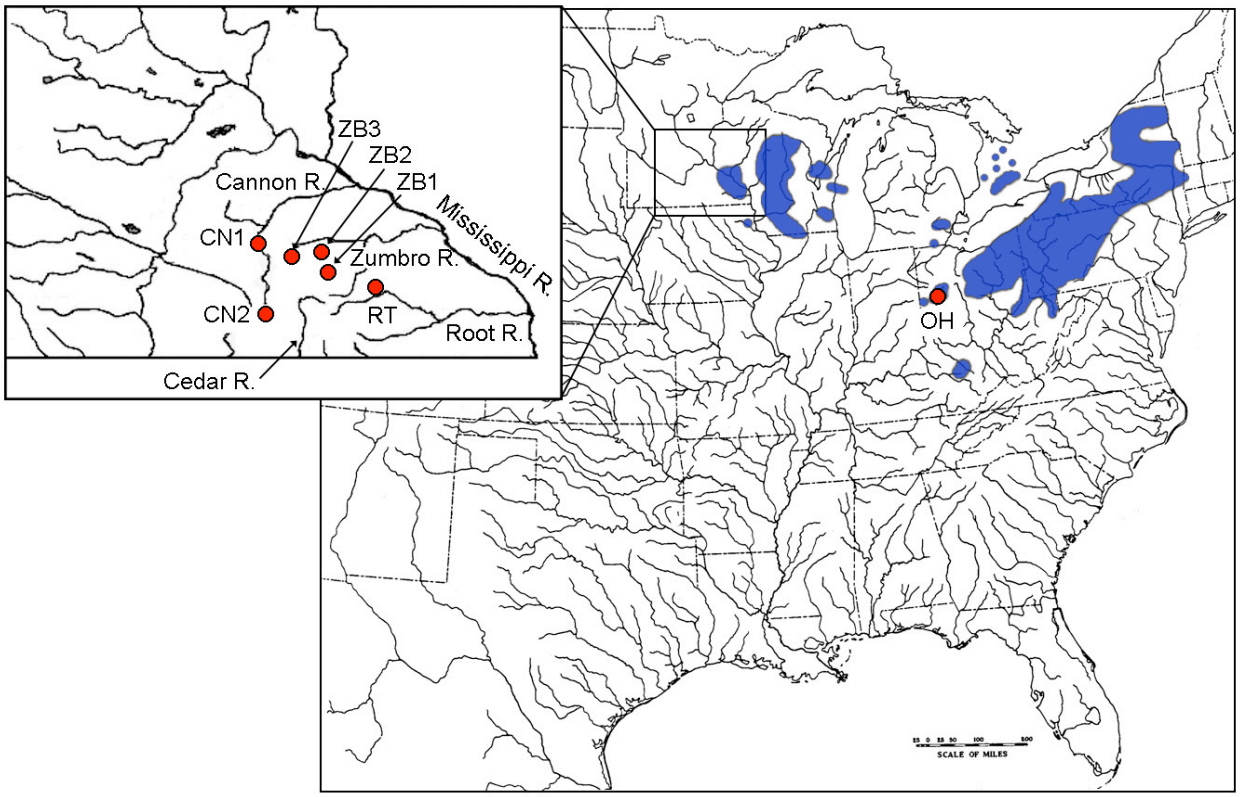

Figure 3. Map of eastern North America and southeastern Minnesota with the approximate distribution of *Clinostomus elongatus* (redside dace). Red dots indicate localities of specimens used in this study. Locality IDs correspond to Table 1.

Clinostomus elongatus has a spotty, widespread distribution in the northern United States and southern Canada (Fig. 3). Populations are confined to small headwater streams from Minnesota, Illinois, and Wisconsin to New York and southern Ontario, Canada (Novinger and Coon 2000). In all parts of its range, populations of the redside dace have dramatically declined due to increased turbidity

of the streams (Becker 1983; Natureserve 2007). The species is presumed extirpated (SX) from Iowa and Maryland, listed as critically imperiled (S1) in Indiana, Michigan and West Virginia, listed as vulnerable (S3) in Kentucky, New York and Wisconsin, and listed as Special Concern by Committee on the Status of Endangered Wildlife in Canada (Canadian Redside Dace Recovery Team 2005; Natureserve 2007). In Minnesota the redside dace is distributed in portions of the Cannon, Zumbro and Root rivers (Fig. 3).

Lythrurus umbratilis (redfin shiner) is the most widespread member of the genus and is characterized as having a slender body, terminal mouth, and an overall silvery color with a bluish gray back (Fig. 4) (Becker 1983). The redfin shiner is contained in the genus *Lythrurus* which contains 11 species distributed in eastern North America. Members of the genus have very small scales on the nape; a dorsal fin origin behind the origin of the pelvic fin; a large, oblique and terminal mouth and development of bright red or yellow fins in breeding males (Pramuk et al. 2007).

Figure 4. *Lythrurus umbratilis* (redfin shiner) breeding male collected from the Cedar River Drainage, Mower Co., MN. Photo by the Fish Genetics Laboratory, University of Northern Iowa.

Redfin shiners are typically found in slow moving pools of small headwater streams to medium sized rivers. They are often found in moderately turbid conditions and seem to avoid springs and cool, clear water (NatureServe 2007). In slow flowing, low gradient streams and rivers, *L. umbratilis* schools can be found in pools along the main channel. In faster moving, higher gradient streams they are found in overflow pools and protected inlets off of the main channel (Snelson and Pflieger 1975). They seem to prefer a hard, clean substrate consisting of rock, gravel or sand (Matthews and Heins 1984). Redfin

shiners spawn in late summer over centrarchid nests including orange-spotted sunfish (*Lepomis humilis*) and longear sunfish (*Lepomis megalotis*), but mainly green sunfish (*Lepomis cyanellus*). Aggregations of as many as 100 males have been observed over green sunfish nests with males and many females on the periphery (Becker 1983). The diet of *L. umbratilis* consists of both aquatic and terrestrial insects, and other small animals when available. They also feed extensively on filamentous algae as well as other aquatic plants (Becker 1983).

Lythrurus umbratilis is distributed from southeastern Ontario, western New York and Pennsylvania; west to southeastern Wisconsin and southeastern Minnesota; and south to southern Louisiana and western Texas and Oklahoma (Fig. 5) (Lee et al. 1980). The redfin shiner is listed as secure (S5) in Illinois, Kansas, Louisiana, Mississippi, Oklahoma, and Tennessee; apparently secure (S4) in Arkansas, Indiana, Iowa, Kentucky, Michigan and Ontario; vulnerable (S3) in West Virginia; imperiled (S2) in Texas, Wisconsin and New York and critically imperiled (S1) in Pennsylvania (NatureServe 2007). It is not ranked or under review (SNR) in Minnesota, Missouri and Ohio. In Minnesota the redfin shiner is distributed in portions of the Zumbro, Root, Upper Iowa and Cedar rivers (Fig. 3).

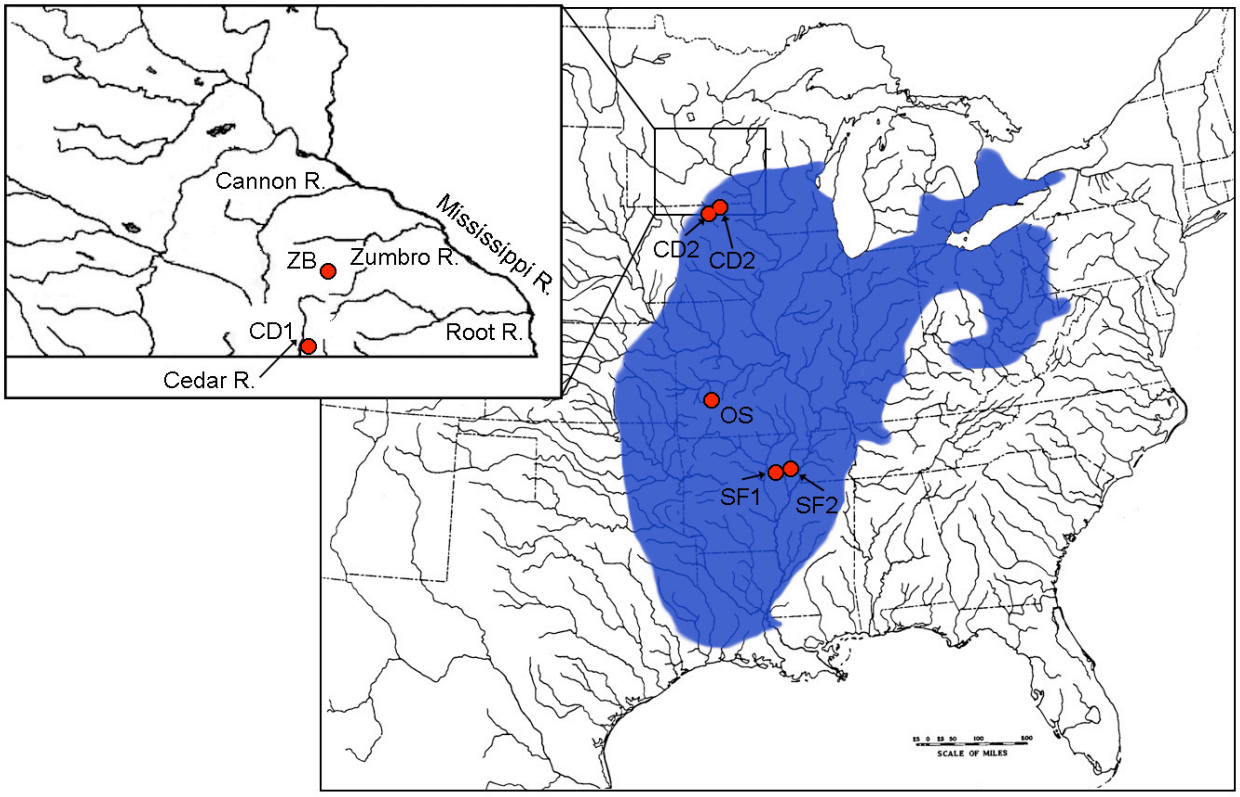

Figure 5. Map of eastern North America and southeastern Minnesota with the approximate distribution of *Lythrurus umbratilis* (redfin shiner). Red dots indicate localities of specimens used in this study. Locality IDs correspond to Table 2.

Notropis nubilus (Ozark minnow) is a member of the genus *Notropis* commonly referred to as shiners. Ozark minnows are recognized by a large eye and blunt snout that extends beyond the mouth (Pflieger 1975; Becker 1983). Their sides are typically silvery with a dusky stripe that extends anteriorly onto the head and around the tip of the snout above the lip (Fig. 6). They average 65 – 70 mm in standard length (Glazier and Taber 1980).

Figure 6. *Notropis nubilus* (Ozark minnow) breeding male collected from the Cedar River Drainage, Mower Co., MN. Photo by the Fish Genetics Laboratory, University of Northern Iowa.

The Ozark minnow is commonly found in streams of 3rd order or less, with clear sandy and rocky bottoms in pools just below riffles or in the backwaters that are protected (Lee et al. 1980; Page and Burr 1991; Natureserve 2007). They typically live in schools near the bottom (Pflieger 1975) where there is a strong and permanent flow with little sediment disturbance (Becker 1983). They spawn in shallow depressions approximately 1 – 20 cm deep in loose gravel from late April to early July (Fowler et al. 1984). They have also been observed spawning in very shallow water 1 – 2 cm deep. Breeding males develop a yellowish-orange color in their fins and under their head (Fig. 6). Their life span is less than 30 months (Glazier and Tabor 1980). Ozark minnows are primarily herbivorous and have rarely been found with anything other than detritus and periphyton in their digestive tract (Felly and Hill 1983).

Notropis nubilus has a unique, disjunct distribution with a large widespread population in the Ozark Highlands of Missouri, Arkansas, Oklahoma and Kansas and a much smaller disjunct population in the upper Mississippi River Basin including Minnesota, Iowa, Illinois and Wisconsin (Fig. 7). The Ozark minnow is one of the most common minnows in the Ozarks (Pflieger 1975);

however, in tributaries of the upper Mississippi River it is much less common. It has declined in abundance and is extirpated from many localities in the upper Mississippi River Basin resulting from agricultural activities increasing the turbidity and siltation of the water (Becker 1983). *Notropis nubilus* is presumed to be critically imperiled (S1) in Kansas; imperiled (S2) in Wisconsin and Illinois; listed as vulnerable (S3) in Minnesota and Iowa (Natureserve, 2007). In Minnesota the Ozark minnow is distributed in portions of the Zumbro, Root and Cedar rivers (Fig. 7).

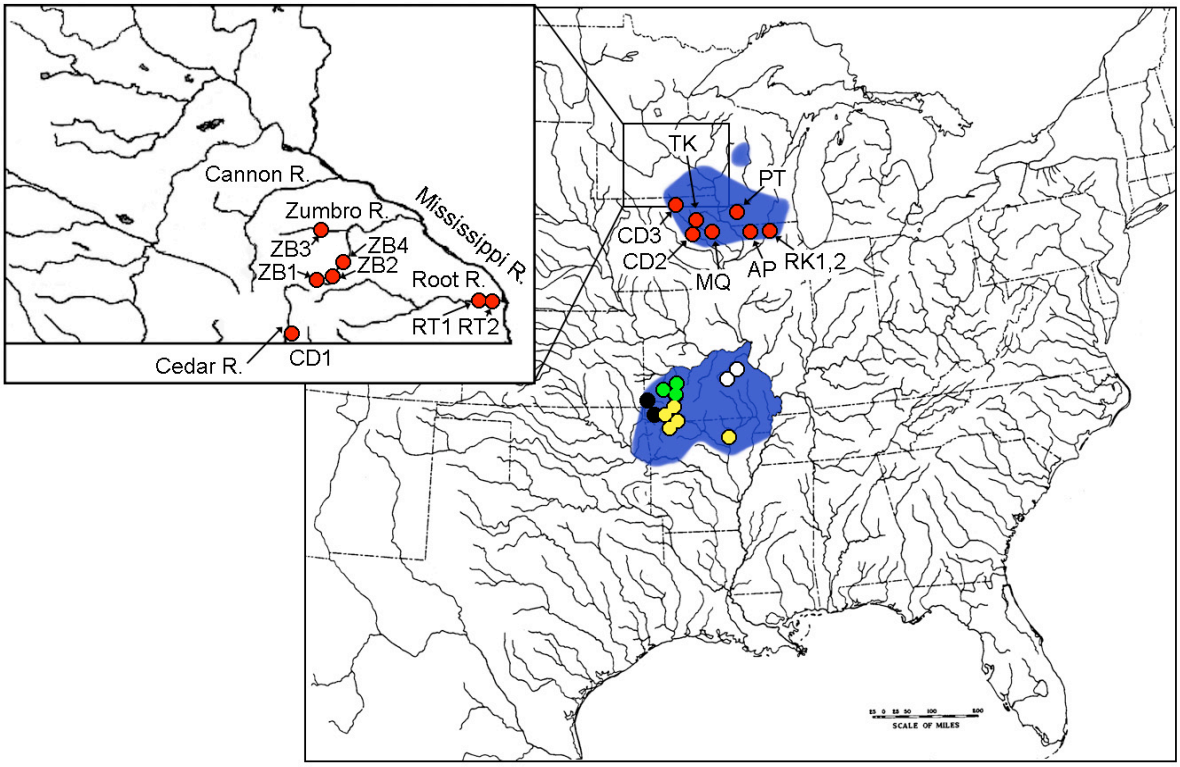

Figure 7. Map of eastern North America and southeastern Minnesota with the approximate distribution of *Notropis nubilus* (Ozark minnow). Red dots indicate localities of specimens in the upper Mississippi River Basin, white dots = MC, yellow dots = WT, green dots = OS and black dots = AR. Locality IDs correspond to Table 3.

The objective of this study is to utilize genetic data to establish a framework for conservation efforts on *Clinostomus elongatus*, *Lythrurus umbratilis* and *Notropis nubilus* within Minnesota. The results of this study: 1) Determine the amount of diversity and limits of species boundaries within each group. 2) Define evolutionary units within Minnesota for directing preservation of genetic diversity within each species. 3) Determine demographic patterns of diversity within each unit. 4) Make recommendations for conservation strategies. Minnesota's CWCS calls for " improved scientific knowledge about species in greatest conservation need" and identifies research on populations of

SGCN as a Priority Conservation Action. This project benefits SGCN as identified by Minnesota's CWCS by determining the population genetic structure of these fishes to help establish a framework for better management. Specifically, this project meets Goal II, improved scientific knowledge about SGCN, Strategy II B, research on populations of SGCN under the Priority Conservation Actions in Minnesota's CWCS.

MATERIALS AND METHODS

Material Examined and DNA extraction

Specimens of *Clinostomus elongatus* were collected from six localities, *Lythrurus umbratilis* from four localities and *Notropis nubilus* from eight localities from all drainages in which they occur in southeastern Minnesota (Figs. 3, 5, 7; Tables 1-3). All specimens were collected using standard seining techniques; all necessary collecting permits were obtained. Fishes were anesthetized in MS 222 and whole specimens were preserved in 95% EtOH for DNA work. Samples were transported to the fish genetics laboratory at the University of Northern Iowa for collection of molecular data. All specimens have been deposited in the Bell Museum of Natural History Fish Collection, University of Minnesota (Tables 1-3). Tissue specimens from representative populations from across the entire range of each species were obtained from the Bell Museum of Natural History Fish Collection, University of Minnesota (Figs. 3, 5, 7; Tables 1-3). Genomic DNA was extracted from muscle tissue and fin clips using QIAamp^{TM} tissue extraction kits (Qiagen Inc.) following manufacturer's instructions.

DNA Sequencing

The complete mitochondrial cytochrome *b* (cyt*b*) gene was amplified using polymerase chain reaction (PCR). PCRs were performed in a total volume of 25 μl containing 5 – 10 ng DNA, 1.2 μM of each primer, 1X *Taq* salts, 3.0 mM $MgCl^2$, 0.4 μM dNTPs, and 1.25 units of *Taq* DNA polymerase (GoTaq Green Master Mix; Promega Corp.). The following thermal profile was used: initial denaturation at 94°C (3 min); 35 cycles of 94°C (10 sec), 50°C (20 sec), 72°C (20 sec); and a final extension at 72°C (10 min) before termination of the reaction at 4°C. The entire gene was amplified using the heavy strand primer HA(16249) [5'-CAA CGA TCT CCG GTT TAC AAG AC-3'] and the light strand primer LA(15058) [5'-GTG ACT TGA AAA ACC ACC GTT G-3'] (Schmidt et al. 1998). Amplification products were purified using ExoSAP-IT (USB corp.) following manufacturer's instructions. Amplification primers were used for sequencing. Automated sequencing was performed using Big Dye (Perkin Elmer) terminator cycle sequencing on an ABI 3730xl DNA analyzer at

Macrogen, Seoul, Korea. Both strands were sequenced. Sequences were checked for accuracy of base determination and assembled using the computer program Sequencher 4.0 (Gene Codes Corp., Ann Arbor, MI). All sequences will be deposited in GenBank (http://www.ncbi.nlm.nih.gov/Genbank).

Table 1. *Clinostomus elongatus* specimens examined. The specimens used in this study are listed with locality ID, number of specimens from each locality, collection locality information and voucher number. JFBM = Bell Museum of Natural History Fish Collection, University of Minnesota.

ID	N	Locality	County	State	Drainage	Latitude / Longitude	Voucher number
ZB1	9	North Branch Middle Fork Zumbro River	Goodhue	MN	Zumbro River	44.11.870 / 92.48.721	JFBM 45546
ZB2	15	Silver Creek	Goodhue	MN	Zumbro River	44.16.155 / 92.52.650	JFBM 45545
ZB3	9	North Fork Zumbro River	Goodhue	MN	Zumbro River	—	JFBM 45562
RT	15	Bear Creek	Fillmore	MN	Root River	43.48.83 / 92.13.52	JFBM 45553
CN1	5	Little Cannon River	Goodhue	MN	Cannon River	44.28.17 / 92.56.00	JFBM 45565
CN2	10	Little Cannon River	Goodhue	MN	Cannon River	44.20.55 / 92.57.27	JFBM 45563
OH	4	Kings Creek	Champaign	OH	Big Miami River	40.09.05 / 83.44.25	JFBM 45570

Table 2. *Lythrurus umbratilis* specimens examined. The specimens used in this study are listed with locality ID, number of specimens from each locality, collection locality information and voucher number. JFBM = Bell Museum of Natural History Fish Collection, University of Minnesota.

ID	N	Locality	County	State	Drainage	Latitude / Longitude	Voucher number
CD1	17	Otter Creek	Mower	MN	Cedar River	43.31.230 / 92.54.798	JFBM 45543
CD2	1	Otter Creek	Mitchell	IA	Cedar River	43.29.258 / 92.56.521	JFBM 45540
CD3	3	Little Cedar River	Mitchell	IA	Cedar River	43.28.855 / 92.45.137	JFBM 45541
ZB	4	North Branch Middle Fork Zumbro River	Goodhue	MN	Zumbro River	44.11.870 / 92.48.721	JFBM 45548
SF1	4	Village Creek	Cross	AR	St. Francis River	—	JFBM 45568
SF2	6	Village Creek	Cross	AR	St. Francis River	35.08.21 / 90.41.34	JFBM 42517
OS	4	Pomme de Terre River	Polk	MO	Osage River	37.26.48 / 93.14.53	JFBM 39027

Table 3. *Notropis nubilus* specimens examined. The specimens used in this study are listed with locality ID, number of specimens from each locality, collection locality information and voucher number. JFBM = Bell Museum of Natural History Fish Collection, University of Minnesota.

ID	N	Locality	County	State	Drainage	Latitude / Longitude	Voucher number
CD1	22	Otter Creek	Mower	MN	Cedar River	43.30.391 / 92.54.984	JFBM 45542
CD2	9	Lime Creek	Buchanan	IA	Cedar River	42.22.188 / 91.57.234	JFBM 45552
CD3	10	Otter Creek	Mitchell	IA	Cedar River	43.29.258 / 92.56.521	JFBM 45540
CD4	5	Otter Creek	Mower	MN	Cedar River	—	JFBM 31417
ZB1	19	Salem Creek	Dodge	MN	Zumbro River	43.57.938 / 92.44.308	JFBM 45549
ZB2	3	South Fork Zumbro River	Olmstead	MN	Zumbro River	43.55.499 / 92.38.274	JFBM 45544
ZB3	9	North Branch Middle Fork Zumbro River	Goodhue	MN	Zumbro River	44.11.870 / 92.48.721	JFBM 45547
ZB4	5	South Fork Zumbro River	—	MN	Zumbro River	—	JFBM 45564
RT1	3	Riceford Creek	Houston	MN	Root River	43.36.26 / 91.42.44	JFBM 45554
RT2	1	Riceford Creek	Houston	MN	Root River	43.36.265 / 91.42.391	JFBM 45561
TK	11	Volga River	Fayette	IA	Turkey River	42.51.710 / 91.45.741	JFBM 45550
MQ	9	South Fork Maquoketa River	Buchanan	IA	Maquoketa River	42.37.206 / 91.40.026	JFBM 45551
RK1	7	Yellow Creek	Stephenson	IL	Rock River	42.15.074 / 89.37.240	JFBM 45555
RK2	9	North Kinnikinnicki River	Winnebago	IL	Rock River	42.27.017 / 88.56.063	JFBM 45557
PT	10	Platte River	Grant	WI	Platte River	45.51.637 / 90.35.152	JFBM 45560
AP	10	South Fork Apple River	Jo Davies	IL	Apple River	42.25.36 / 90.01.100	JFBM 45558
GS	10	Big Piney River	Texas	MO	Gasconade River	37.13.11 / 92.00.17	JFBM 40926
OS1	5	Pomme de Terre River	Hickory	MO	Osage River	37.56.15 / 93.18.48	JFBM 37850

Table 3. continued…

ID	N	Locality	County	State	Drainage	Latitude / Longitude	Voucher number
OS2	1	Pomme de Terre River	Polk	MO	Osage River	37.26.48 / 93.14.53	JFBM 39030
OS3	2	Pomme de Terre River	Polk	MO	Osage River	37.40.30 / 93.22.27	JFBM 45566
WT1	10	War Eagle Creek	Madison	AR	White River	—	JFBM 30535
WT2	5	North Fork White River	Ozark	MO	White River	36.45.00 / 92.09.26	JFBM 39476
WT3	4	James River	Stone	MO	White River	36.55.57 / 93.23.21	JFBM 40537
WT4	8	Strawberry River	Independence	MO	White River	36.05.59 / 91.34.41	JFBM 45571
WT5	1	Spring River	Fulton	AR	White River	—	JFBM 45569
WT6	7	Kings River	Carrol	AR	White River	—	JFBM 30450
MC1	5	Big River	Washington	MO	Meramec River	—	JFBM 45573
MC2	3	Reis Biological Station	Crawford	MO	Meramec River	—	JFBM 45572
AR1	4	Elk River	McDonald	MO	Arkansas River	36.37.26 / 94.35.25	JFBM 45574
AR2	3	Elk River	McDonald	MO	Arkansas River	36.37.25 / 94.35.26	JFBM 37899
AR3	1	Shoal Creek	Newton	MO	Arkansas River	37.01.39 / 94.33.38	JFBM 45567

Microsatellite Analysis

Due to the time frame and budget of the project we were not able to develop specific primers for microsatellite loci for each species included in the study. In addition, published primer sets for mircrosatellite loci for these species are not available. However, primer pairs developed in one species can often be used in closely related species because primer sites are generally highly conserved. Microsatellite primer sets for closely related species are available; 17 loci for *Campostoma anomalum* (Dimsoski et al. 2000), 14 loci for *Pimephales promelas* (Ardren et al. 2002; Bessert and Orti 2003), 11 loci for *Rhynichthys cataractae* (Girard and Angers 2006), 29 loci for *Semotilus atromaculatus*

(Skalski and Grose 2006) and eight loci for divergent lineages of cyprinid fishes in the subfamily Leusicinae (Turner et al. 2004).

A total of 79 primer pairs were initially screened for each species for ability to amplify by PCR, evidence of variability and ability to score. Seven individuals from across the range of each species and a negative control were used for screening. PCRs were performed in a total volume of 25 μl containing 5 – 10 ng DNA, 0.5 μM of each primer, 1X *Taq* salts, 2.5 mM $MgCl^2$, 0.4 μM dNTPs, and 1.25 units of *Taq* DNA polymerase (GoTaq Green Master Mix; Promega Corp.). The following thermal profile was used for all amplifications: initial denaturation at 94°C (2 min.); 40 cycles of 94°C (30 sec.), 50°C (30 sec.), 72°C (1 min.); and a final extension at 72°C (7 min.) before termination of the reaction at 4°C. PCR products were visualized on a 1.8% agarose gel.

Loci that yielded scorable, polymorphic PCR products were then amplified and fluorescently labeled for all individuals for each species using a single-tube, single-reaction nested PCR method (Schuelke 2000; Boutin-Ganache et al. 2001). This reaction is performed with three primers: a sequence-specific forward primer with a M13 (5'-CAC GAC GTT GTA AAA CGA C-3') tail at its 5' end, a sequence-specific reverse primer and a universal florescent-labeled M13 (5'-FAM CAC GAC GTT GTA AAA CGA C-3') primer. The M13 primer was labeled with either HEX or FAM. Nested PCRs were performed in a total volume of 25 μl containing 5 – 10 ng DNA, 1.5 pmol labeled M13 primer and reverse primer, 0.1 pmol M13-tailed forward primer, 1X *Taq* salts, 2.5 mM $MgCl^2$, 0.4 μM dNTPs, and 1.25 units of *Taq* DNA polymerase (GoTaq Green Master Mix; Promega Corp.). The following thermal profile was used for all nested amplifications: initial denaturation at 94°C (2 min.); 10 cycles of 94°C (20 sec.), 50°C (20 sec.), 72°C (30 sec.); 30 cycles of 94°C (20 sec.), 48°C (20 sec.), 72°C (30 sec.) and a final extension at 72°C (10 min.) before termination of the reaction at 4°C. Nested PCR products were sent to the DNA Facility of the Iowa State University Office of Biotechnology for genotyping on an ABI 3100 Genetic Analyzer (Applied Biosystems). Allele sizes were determined using Peak Scanner v1.0 (Applied Biosystems).

DNA Sequence Variation and Phylogenetic analyses

The number of variable and parsimony-informative sites for the cyt*b* sequence data set was calculated using GARLI 0.951 (Zwickl 2006) for each species. Uncorrected percent pairwise distances (*p*) were calculated using PAUP*4.0b10 (Swofford 2001) to identify unique haplotypes. Only unique haplotypes were used for phylogenetic analyses. Nucleotide diversity was calculated using ARLEQUIN 3.1 (Excoffier et al. 2005)

Phylogenetic analyses were performed on the cyt*b* sequence data set for each species to determine the relationships among haplotypes. Sequences for all outgroup taxa were downloaded from GenBank; numbers are included in parentheses. Based on the phylogenetic hypothesis of Simons et al. (2003), *Richardonius balteatus* (AY096011) was included as an outgroup taxon for phylogenetic analyses of *Clinostomus elongatus*. Based on the phylogenetic hypothesis of Schmidt et al. (1998) and Pramuk et al. (2007) members of the genus *Lythrurus* were included as outgroup taxa for phylogenetic analyses of *L. umbratilis*; *L. ardens* (U17268), *L. atrapiculus* (U17271), *L. bellus* (U17275), *L. fumeus* (U17269), *L. lirus* (U17273), and *L. roseipinnis* (X66256). Based on the phylogenetic hypothesis by Bielawski and Gold (2001) all members of the subgenus *Notropis* were included as outgroup taxa for phylogenetic analyses of *N. nubilus*: *N. amabilis* (AF352269), *N. amoenus* (AF352270), *N. ariommus* (AF352271), *N. atherinoides* (AF352273), *N. boops* (AF352261), *N. candidus* (AF352275), *N. chrosomus* (AF352262), *N. edwardraneyi* (AF352263), *N. girardi* (AF352276), *N. jemezanus* (AF352277), *N. longirostris* (AF352264), *N. nubilus* (AF352265), *N. oxyrhynchus* (AF352278), *N. perpallidus* (AF352279), *N. photogenis* (AF352281), *N. potteri* (AF352266), *N. scepticus* (AF352283), *N. shumardi* (AF352284), *N. stilbius* (AF352286), *N. telescopus* (AF352290), *N. texanus* (AF352267), *N. volucellus* (AF352268).

Parsimony analyses were performed using the heuristic search option, 100 random addition sequence replicates, and tree-bisection-reconnection (TBR) algorithm in PAUP*. All bases were equally weighted and maximum number of trees saved was set to 10,000. Parsimony trees were evaluated using summary values reported by PAUP*. Support for nodes was evaluated by calculating bootstrap values (Felsenstein 1985) using 100 pseudoreplicate bootstraps with a full heuristic search, simple step-wise addition option and TBR.

MrModeltest 2.2 (Nylander 2004) was used to determine the likelihood model that provided the simplest explanation of the data for each species (Posada and Crandall 2001) using the Akaike Information Criterion, AIC (Posada and Buckley 2004). Likelihood analyses were performed using GARLI 0.951 (Zwickl 2006) with the model determined by AIC. Analyses were terminated after 10,000 generations without an improvement in the overall tree topology. Support was evaluated using 100 pseudoreplicate bootstraps (Felsenstein 1985) with each repetition terminated after 10,000 generations without topology improvement.

Bayesian analyses were carried out using MrBayes 3.1 (Ronquist and Huelsenbeck 2003) using the model determined by AIC, random starting tree, uniform interval priors except base composition, which assumed a Dirichlet prior. Markov chain Monte Carlo was run with four chains for 2,000,000 generations. Trees were sampled every hundred generations and branch lengths of all sampled trees

were saved. The burn-in, the number of trees generated prior to the Markov chain Monte Carlo reaching stationarity, was determined by plotting the log-likelihood scores of sampled trees against generation time (Huelsenbeck and Ronquist 2001). Trees generated after the burn-in were used to generate a 50% majority rule consensus tree. The percentage of times each node occurs among these trees is interpreted as the posterior probability of that node (Huelsenbeck and Ronquist 2001).

Net between-group mean distances were calculated using the formula: $\delta = \delta_{xy} - (\delta_x + \delta_y) / 2$, where δ_x and δ_y are the mean distances within groups x and y and δ_{xy} is the average distance between groups x and y (Nei and Li 1979). This correction is important for recently diverged groups so that divergence time is not overestimated (Edwards 1997). Mean sequence divergence within each group was calculated. Distances and standard error, using 500 bootstrap replicates, were calculated using the Kimura 2-parameter (K2P) model in MEGA3 (Kumar et al. 2004).

Microsatellite Data Analysis

Exact tests for gametic linkage disequilibrium for all pairs of loci and for deviation from expected Hardy-Weinberg equilibrium (HWE) for each locus and population for each species was performed using GENEPOP 3.3 (Raymond and Rousset 1995). Gametic linkage disequilibrium is the non-random association between alleles of two loci. The null hypothesis (H_O) is that genotypes at one locus are independent of genotypes at a second locus. Deviation from H_O suggests that there is linkage disequilibrium. Hardy-Weinberg equilibrium implies that genotype frequencies are constant from generation to generation. Genetic diversity was estimated as mean expected (H_E) and observed (H_O) heterozygosities under HWE assumptions in GENEPOP and allelic richness per locus (A_R; El Mousadik and Petit 1996) using FSTAT 2.9.3.2 (Goudet 2001). Allelic richness measures allelic diversity per locus corrected for different sample sizes. The number of private alleles (N_{PA}), alleles present in only one of many populations sampled, was determined for each population. Groups were either defined by drainage or based on phylogenetic analyses.

Population Genetic Structure

Population subdivision (F_{ST}) was estimated using pairwise distances under the K2P model using ARLEQUIN 3.1 for both the mtDNA and microsatellite data sets. We tested the null hypothesis of no differentiation among groups ($F_{ST} = 0$) using the permutation test. Significant F_{ST} values provide evident evidence of lack of gene flow and can support or reject the validity of non-monophyletic groups as distinct evolutionary lineages.

A nested analysis of molecular variance (AMOVA) (Excoffier et al. 1992) was used to test the spatial structure of genetic variation within each species for both the mtDNA and microsatellite data sets separately. Pairwise distances were used and significance of each estimator was based on 10000 permutations. All analyses were run in ARLEQUIN 3.1.

The Bayesian population assignment protocol performed with the program STRUCTURE (Pritchard et al. 2000) was used to infer the number of populations (K) and to assign individuals to populations based on their genotypes without the need *a priori* to define population units. This test was used to determine if the variation in the microsatellite data was consistent with the results of the mtDNA anlyses or if greater, fine-scale population structure could be detected. We estimated the number of genetic clusters (K) by conducting five independent runs each for $K = 1 – 10$ with 10^6 Markov Chain Monte Carlo repetitions, a 10^5 burn-in period and the admixture model of ancestry. The optimal value of K was determined using the method of Pritchard et al. (2000) and the ΔK method described by Evanno et al. (2005).

RESULTS

Clinostomus elongatus

The fragment of the cyt*b* gene, a total of 1109 nucleotides, was sequenced for 55 individuals of *Clinostomus elongatus*. The entire data set contained a total of 113 variable sites of which eight were potentially informative and 105 were apomorphic. Uncorrected *p*-distances within *C. elongatus* ranged from 0.00% - 0.38%. The data set was pruned to include only nine unique haplotypes (Fig. 8).

The model GTR was the best-fit model to the data set based on AIC. The consensus Bayesian trees (harmonic mean –lnL = 3765.21), maximum likelihood tree (-lnL = 1996.53) and parsimony trees (2 equally parsimonious trees, TL = 113, CI = 1.000, RI = 1.000, RC = 1.000) all recovered a monophyletic *Clinostomus elongatus* (Fig. 8). The topologies of the Bayesian, maximum likelihood and parsimony trees were very similar. Within *C. elongatus* there was a single clade containing all haplotypes with little resolution, no geographic structuring and very short branch lengths (Fig. 8).

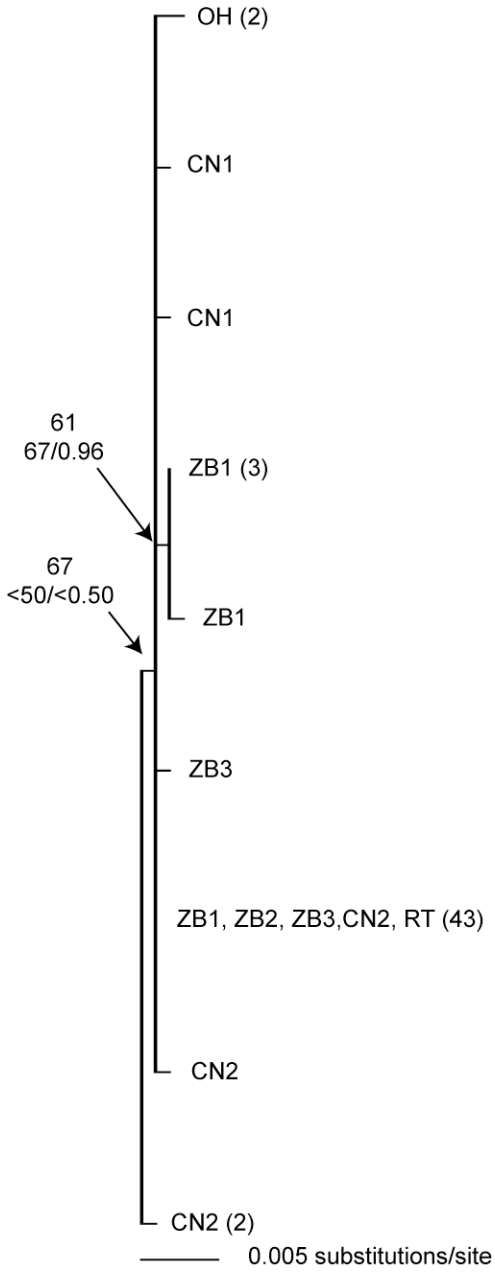

Figure 8. Topology of *Clinostomus elongatus* haplotypes produced in the maximum likelihood analysis for the cyt*b* data set. Numbers above nodes indicate parsimony bootstrap values. Numbers below nodes indicate maximum likelihood boostrap values followed by Bayesian posterior probabilities. Outgroup is not shown. Locality ID corresponds to Table 1. Numbers in parentheses indicated number of individuals with identical haplotypes.

Molecular diversity indices of the cyt*b* data set are listed in Table 4. Although there are nine unique haplotypes within the group the nucleotide diversity is very low.

Table 4. Molecular diversity of the cyt*b* data set for *Clinostomus elongatus* as determined by the phylogenetic analyses.

	n	Number of Private Haplotypes	Nucleotide Diversity ± SD
Clade	55	9	0.0008 ± 0.0006

Of the 79 microsatellite loci screened in *Clinostomus elongatus* 10 were scorable and eight were polymorphic with two or more alleles (Table 5). No significant linkages were found between any pair of loci. The only significant departures from Hardy-Weinberg equilibrium were found in Lco4 for the Cannon River population and Seat207 for the Root River population. In the Zumbro, Root and Cannon river populations six microsatellite loci were polymorphic and two were monomorphic. In the Ohio population seven loci were polymorphic and one was monomorphic. Private alleles were observed in three loci in the Zumbro River: Ppr106, Lco4 and Ca1. In the Root River only one locus, Ppro118, had private alleles and in the Cannon River private alleles were observed in four loci: Lco4, Rhca23, Ppro118 and Ca1. Four loci had private alleles in the Ohio population: Lco1, Lco4, Ca1 and Seat206. The mean allelic richness for the Zumbro and Root rivers was similar (1.681 and 1.700; Table 5) and slightly higher in the Cannon River and Ohio (2.026 and 2.161; Table 5).

Net-between group mean distances for the cyt*b* data set and within group distances for both the cyt*b* and microsatellite data sets are listed in Table 6. These data revealed that there is very little diversity in the cyt*b* data and greater diversity in the microsatellite data. Population subdivision measured as pairwise F_{ST} revealed little differentiation between the Cannon and Zumbro rivers in the cyt*b* data set (Table 6). The microsatellite data has less genetic genetic differentiation than the cyt*b* data indicating a greater amount of gene flow.

Table 5. Summary of microsatellite genetic variation in *Clinostomus elongatus* including: number of individuals sampled (*n*); number of alleles in each population (*k*); allelic richness (A_R); number of private alleles (N_{PA}); *P* value of exact tests for deviation from expected Hardy-Weinberg equilibrium (HWE); expected (H_E) and observed (H_O) heterozygosities. Asterisk indicates deviation from HWE. Groups are based on the results of the cluster analyses (Figs. 9, 10). Specific locality IDs correspond to Table 1.

Locus		Zumbro River (ZB)	Root River (RT)	Cannon River (CN)	Ohio (OH)
Ppr106	*n*	33	15	15	4
(Ardren et al. 2002)	*k*	3	3	4	4
Size Range: 355 – 386 bp	A_R	2.244	1.386	1.626	2.557
Alleles: 6	N_{PA}	1	0	0	0
	HWE	0.1443	1	1	0.3094
	H_E	19.9231	2.8621	4.5517	2.8571
	H_O	16	3	5	2
Lco1	*n*	33	15	15	4
(Turner et al. 2004)	*k*	2	3	1	4
Size Range: 253 – 265 bp	A_R	1.842	2.120	1.000	3.000
Alleles: 4	N_{PA}	0	0	0	1
	HWE	0.7214	0.6487	-	0.7622
	H_E	15.7692	8.6897	-	3.2857
	H_O	17	11	-	4
Lco4	*n*	33	15	15	4
(Turner et al. 2004)	*k*	2	2	3	2
Size Range: 238 – 258 bp	A_R	1.323	1.612	2.312	1.971
Alleles: 5	N_{PA}	1	0	1	1
	HWE	0.2197	0.4587	*0.0470	0.3140
	H_E	5.5385	4.9655	9.4828	2.2857
	H_O	4	4	13	4
Rhca23	*n*	33	14	13	2
(Girard and Angers 2006)	*k*	1	2	3	1
Size Range: 299 – 309 bp	A_R	1.000	1.538	2.347	1.000
Alleles: 3	N_{PA}	0	0	1	0
	HWE	-	-	0.8541	-
	H_E	-	4.3103	8.3600	-
	H_O	-	5	8	-

Table 5. continued…

Locus		Zumbro River (ZB)	Root River (RT)	Cannon River (CN)	Ohio (OH)
Ppro118	*n*	33	15	15	4
(Bessert and Orti 2003)	*k*	7	4	9	4
Size Range: 217 – 298 bp	A_R	2.625	2.618	3.291	2.771
Alleles: 12	N_{PA}	0	1	4	0
	HWE	*0.0246	0.2802	0.8155	0.3173
	H_E	23.2462	10.7241	13.0344	3.0000
	H_O	18	13	12	3
Ca1	*n*	33	15	15	4
(Dimsoski et al 2000)	*k*	3	1	3	3
Size Range: 125 – 159 bp	A_R	1.920	1.000	2.569	2.557
Alleles: 9	N_{PA}	2	0	3	2
	HWE	0.5116	-	0.2699	0.3150
	H_E	14.6615	-	10.1724	2.8571
	H_O	16	-	9	2
Seat206	*n*	33	15	15	4
(Skalski and Grose 2006)	*k*	1	1	1	2
Size Range: 517 – 519 bp	A_R	1.000	1.000	1.000	1.500
Alleles: 2	N_{PA}	0	0	0	1
	HWE	-	-	-	-
	H_E	-	-	-	1.0000
	H_O	-	-	-	1
Seat207	*n*	33	15	15	4
(Skalski and Grose 2006)	*k*	2	3	3	2
Size Range: 124 – 129 bp	A_R	1.490	2.317	2.059	1.929
Alleles: 3	N_{PA}	0	0	0	0
	HWE	1	*0.0156	0.4074	1
	H_E	8.6154	9.4138	7.7241	2.1429
	H_O	10	14	10	3
Average for all loci	A_R	1.681	1.700	2.026	2.161
	H_E	10.700	5.121	6.666	2.179
	H_O	10.125	6.250	7.125	2.375

Table 6. On diagonals (in **bold**) are within group average genetic distances [and standard error] for *Clinostomus elongatus*. Below each diagonal are net between-group mean genetic distances [and standard error] between populations for the cyt*b* data only. Above each diagonal are pairwise F_{ST}, based on pairwise distance. All distances were estimated using the K2P model.

Marker	Drainage	ZB	OH	CN	RT
cyt*b*	ZB	**0.000 [0.000]**	0.843	0.099	0.761
	OH	0.002 [0.001]	**0.000 [0.000]**	0.626	1.000
	CN	0.000 [0.000]	0.002 [0.001]	**0.001 [0.001]**	0.617
	RT	0.000 [0.000]	0.002 [0.001]	0.000 [0.000]	**0.000 [0.000]**
microsatellite	ZB	**0.266 [0.159]**	0.358	0.184	0.279
	OH	---	**0.484 [0.305]**	0.325	0.418
	CN	---	---	**0.333 [0.199]**	0.206
	RT	---	---	---	**0.273 [0.166]**

Across the four local populations the AMOVA of the cyt*b* data set revealed that defining groups by regions, upper Mississippi River Basin and Ohio, did not explain the variation among haplotypes (F_{CT} = 0.61094, $P < 0.258$, Table 7A). The AMOVA of the microsatellite data was consistent with this result (F_{CT} = 0.20116, $P < 0.239$, Table 7C). Most of the variation among haplotypes in the cyt*b* data set was explained by differences among drainages (F_{ST} = 0.61141, $P = < 0.001$, Table 7B). The microsatellite data revealed some variation among drainages (F_{ST} = 0.25428, $P = < 0.001$, Table 7D), with most of the variation explained within drainages.

The Bayesian admixture procedure implemented in STRUCTURE (Pritchard et al. 2000) showed an incremental increase in the likelihood [Pr(X/K)] as the number of genetic clusters in the model increased from one to four. After four, there was a slight decrease in the likelihood as the number of clusters used in the model increased to K = 10 (Fig. 9). Following the method of Evanno et al. (2005), we determined the distribution of ΔK to have a strong modal value at K = 4 (Fig. 9). This indicated that the highest level of population structure exists in four genetic clusters.

The membership coefficients of each individual in these clusters for K = 4, along with corresponding localities are shown in Fig. 10. This revealed a pattern where individuals from each drainage tended to cluster together. This suggests that there is isolation by drainage and little gene flow between them.

Table 7. AMOVA variance components for *Clinostomus elongatus*, percentage variation explained at each spatial level and fixation indices for **A**) cyt*b* data with groups defined by Ohio and upper Mississippi River Basin, **B**) cyt*b* data with populations defined by drainage, **C**) microsatellite data with groups defined by Ohio and upper Mississippi River Basin, **D**) microsatellite data with populations defined by drainage.

A)

Source of variation	d.f	Variance components	Percentage variation	Fixation indices
Among groups	1	0.77261 Va	61.09	F_{CT} = 0.61094 (P<0.258)
Among drainages within groups	2	0.26653 Vb	21.08	F_{SC} = 0.54171 (P<0.001)
Within drainages	51	0.22548 Vc	17.83	
Total	54	1.26461		F_{ST} = 0.82170 (P<0.001)

B)

Source of variation	d.f	Variance components	Percentage variation	Fixation indices
Among drainages	3	0.35478 Va	61.14	
Within drainages	51	0.22548 Vb	38.86	
Total	54	0.58025		F_{ST} = 0.61141 (P<0.001)

C)

Source of variation	d.f	Variance components	Percentage variation	Fixation indices
Among groups	1	0.44960 Va	20.12	F_{CT} = 0.20116 (P<0.239)
Among drainages within groups	2	0.39641 Vb	17.74	F_{SC} = 0.22202 (P<0.001)
Within drainages	130	1.38903 Vc	62.15	
Total	133	2.23504		F_{ST} = 0.37852 (P<0.001)

D)

Source of variation	d.f	Variance components	Percentage variation	Fixation indices
Among drainages	3	0.47364 Va	25.43	
Within drainages	130	1.38903 Vb	74.57	
Total	133	1.86267		F_{ST} = 0.25428 (P<0.001)

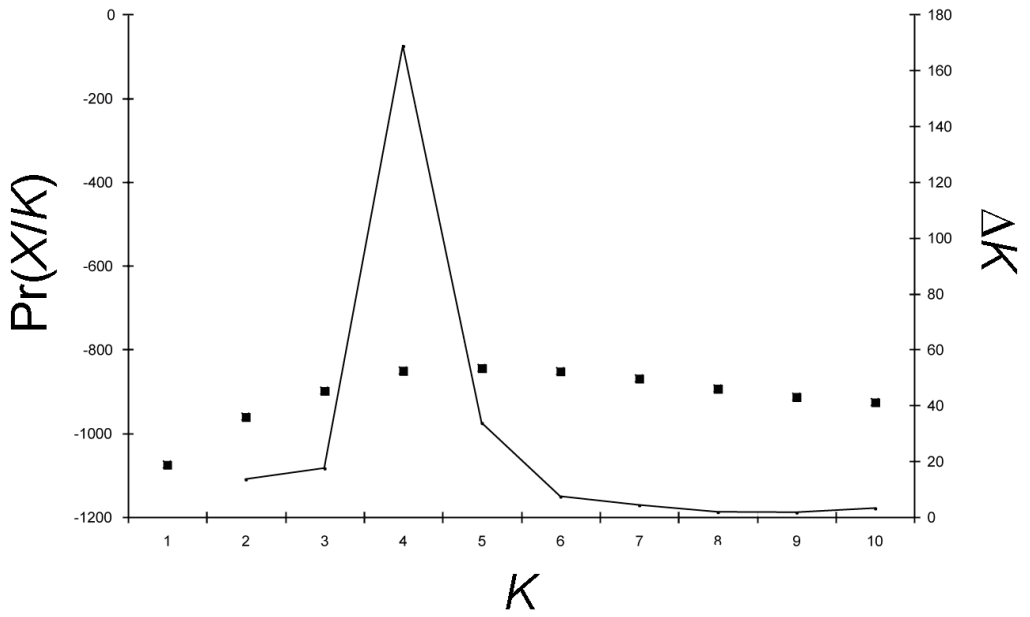

Figure 9. Plot of the number of genetically discrete populations (*K*) in *Clinostomus elongatus* versus the two optimality criteria: the raw average -Ln likelihood indicated by squares and scaled to the left vertical axis (Pritchard et al. 2000) and Δ*K* (Evanno et al. 2005) indicated by the solid line and scaled to the right vertical axis.

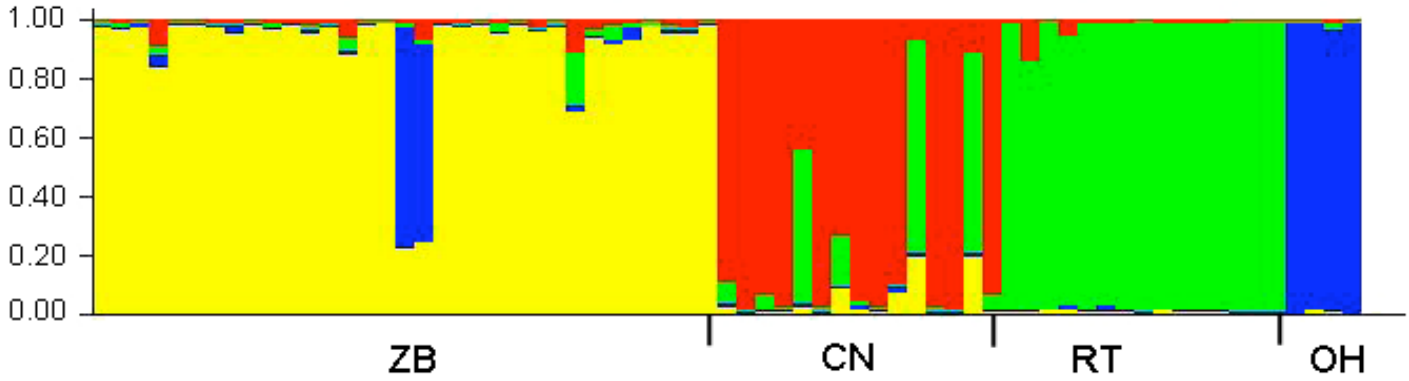

Figure 10. Estimated membership coefficients in *Clinostomus elongatus* based on admixture analyses for *K* = 4 genetically defined populations for each individual sampled. Vertical axis indicates membership coefficient and the horizontal axis indicates the population of each individual. Locality IDs correspond to Table 1.

Lythrurus umbratilis

The complete cyt*b* gene, a total of 1140 nucleotides, was sequenced for 161 individuals of *Lythrurus umbratilis*. The entire data set contained a total of 301 variable sites of which 204 were potentially informative and 97 were apomorphic. Uncorrected *p*-distances within *L.umbratilis* ranged from 0.00% - 3.98%. The data set was pruned to include only 20 unique haplotypes (Fig. 11).

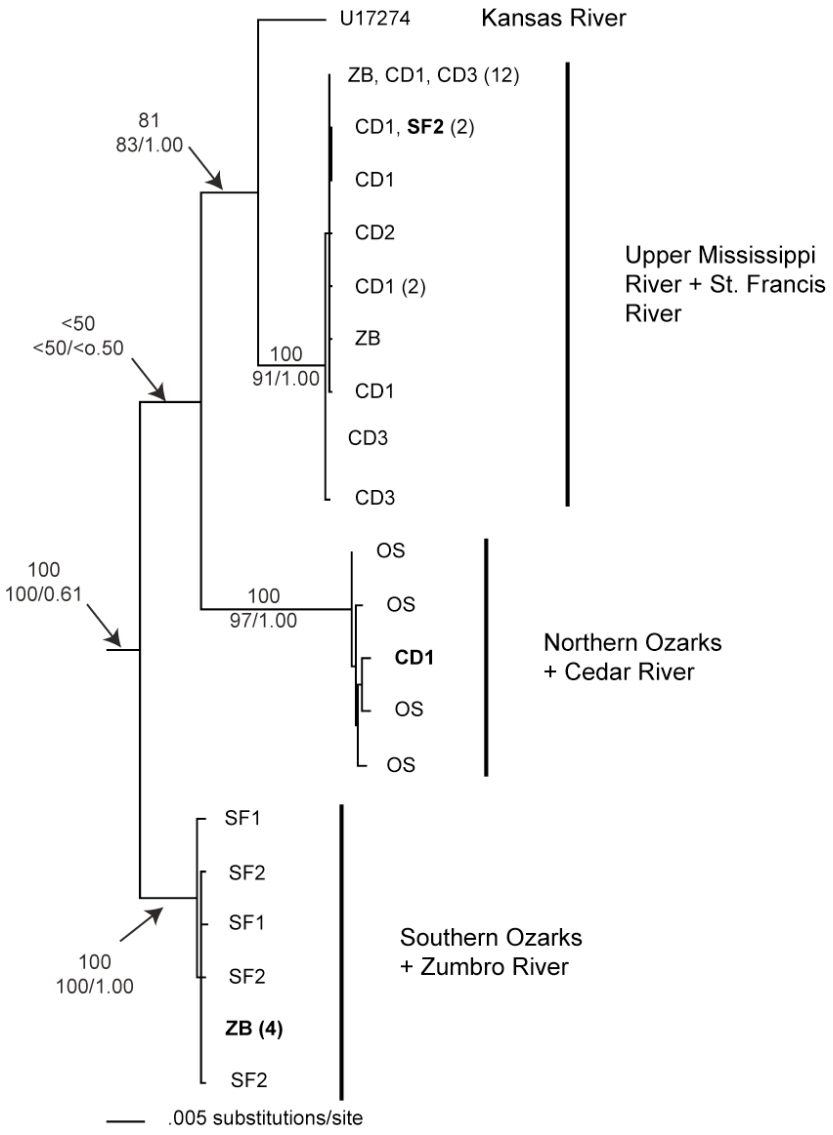

Figure 11. Topology of *Lythrurus umbratilis* haplotypes produced in the maximum likelihood analysis for the cyt*b* data set. Numbers above nodes indicate parsimony bootstrap values. Numbers below nodes indicate maximum likelihood bootstrap values followed by Bayesian posterior probabilities. Outgroups are not shown. Locality ID corresponds to Table 2. Localities in bold represent individuals that do not correspond with the range of the other haplotypes in the clade. Numbers in parentheses indicated number of individuals with identical haplotypes.

The model GTR + Γ was the best fit to the data set based on AIC. The consensus Bayesian trees (harmonic mean –lnL = 7878.62), maximum likelihood tree (-lnL = 4197.74) and parsimony trees (>10,000 equally parsimonious trees, TL = 578, CI = 0.6159, RI = 0.7685, RC = 0.4733) all recovered a monophyletic *Lythrurus umbratilis* (Fig. 11). The topologies of the Bayesian, maximum likelihood and parsimony trees were very similar. The observed differences were within major clades that exhibited short branch lengths and no geographic structuring among haplotypes. Within *L. umbratilis* there were three distinct clades. These clades generally corresponded to geographic regions; however, each clade contained at least one individual from outside the region. The individual from the Kansas River was sister to a clade containing haplotypes from the upper Mississippi River Basin and St. Francis river in the southern Ozarks. Two individuals from the St. Francis River had the same haplotype as an individual from the Cedar River. The northern Ozarks formed a monophyletic group with one individual from the Cedar River. The southern Ozarks formed a monophyletic group that contained four individuals with the same haploytpe from the Zumbro River.

Molecular diversity indices of the cyt*b* data are listed in Table 8. The clade containing the northern Ozarks and Cedar River had the greatest amount of nucleotide diversity within the species. The other clades contained a much lower level of nucleotide diversity.

Table 8. Molecular diversity of cyt*b* data set for *Lythrurus umbratilis* as determined by the phylogenetic analyses.

Clade	n	Number of Private Haplotypes	Nucleotide Diversity ± SD
Kansas River	1	1	---
Upper Mississippi River and St. Francis River	22	6	0.0009 ± 0.0007
Northern Ozarks and Cedar River	5	5	0.0043 ± 0.0029
Southern Ozarks and Zumbro River	11	6	0.0009 ± 0.0007

Net between-group mean and within group distances for the cyt*b* data set are listed in Table 9. These data revealed that there is little within group diversity. The divergence between groups ranged from 0.024 – 0.070 (Table 9). Population subdivision measured as pairwise F_{ST} revealed differentiation among the groups and little gene flow.

Table 9. On diagonals (in **bold**) are within group average genetic distances [and standard error] of the cyt*b* data set for *Lythrurus umbratilis*. Below each diagonal are net between-group mean genetic distances [and standard error] between populations. Above each diagonal are pairwise F_{ST}, based on pairwise distance. All distances were estimated using the K2P model. KR = Kansas River; UMSTF = Upper Mississippi River and St. Francis River; NOCR = Northern Ozarks and Cedar River; SOZR = Southern Ozarks and Zumbro River.

Marker	Drainage	KR	UMSTF	NOCR	SOZR
cyt*b*	KR	**0.000 [0.000]**	0.938	0.724	0.974
	UMSTF	0.033 [0.006]	**0.004 [0.003]**	0.841	0.980
	NOCR	0.068 [0.008]	0.070 [0.008]	**0.014 [0.008]**	0.829
	SOZR	0.044 [0.006]	0.024 [0.004]	0.061 [0.007]	**0.001 [0.001]**

Table 10. AMOVA variance components for *Lythrurus umbratilis*, percentage variation explained at each spatial level and fixation indices for **A**) cyt*b* data with groups defined by upper Mississippi River Basin and Ozarks, **B**) cyt*b* data with populations defined by drainage.

A)

Source of variation	d.f	Variance components	Percentage variation	Fixation indices
Among groups	1	-0.1656 Va	-0.75	F_{CT} = -0.0075 (P<0.288)
Among drainages within groups	3	16.3270 Vb	74.09	F_{SC} = 0.7353 (P<0.001)
Within drainages	34	5.8621 Vc	26.66	
Total	38	22.0368		F_{ST} = 0.73333 (P<0.001)

B)

Source of variation	d.f	Variance components	Percentage variation	Fixation indices
Among drainages	3	23.0965 Va	89.15	
Within drainages	35	2.8100 Vb	10.85	
Total	38	25.9066		F_{ST} = 0.61141 (P<0.001)

Across the four populations the AMOVA of the cyt*b* data revealed that defining groups by regions (upper Mississippi River Basin and Ozarks) did not explain the variation among haplotypes (F_{CT} = -0.0075, P<0.288, Table 10A). Most of the variation among haplotypes in the cyt*b* data was explained by differences among drainages (F_{ST} = 0.61141, P<0.001, Table 10B).

We screened 79 microsatellite loci in *Lythrurus umbratilis*, but were unable to detect any scorable, polymorphic loci. Therefore, no microsatellite analyses were performed for this species.

Notropis nubilus

The complete cyt*b* gene, a total of 1140 nucleotides, was sequenced for 161 individuals of *Notropis nubilus*. The entire data set contained a total of 419 variable sites of which 380 were potentially informative and 38 were apomorphic. Uncorrected *p*-distances within *N. nubilus* ranged from 0.00% - 5.12%. The data set was pruned to include only 71 unique haplotypes (Fig. 12).

The model GTR + I + Γ was the best fit to the data set based on AIC. The consensus Bayesian trees (harmonic mean –lnL = 21510.92), maximum likelihood tree (-lnL = 8710.2989) and parsimony trees (>10,000 equally parsimonious trees, TL = 1746, CI = 0.3402, RI = 0.6909, RC = 0.2350) all recovered a monophyletic *N. nubilus* (Fig. 12). The topologies of the Bayesian, maximum likelihood and parsimony trees were very similar. The observed differences were within major clades that exhibited short branch lengths and no geographic structuring among haplotypes. Within *N. nubilus* there were three distinct clades; a clade containing haplotypes from the western Ozarks, a clade containing haplotypes from the Upper Mississippi River Basin and the northern Ozarks and a clade containing haplotypes from the southern Ozarks (Fig. 12). Within all clades there was little resolution, no geographic structuring and relatively short branch lengths.

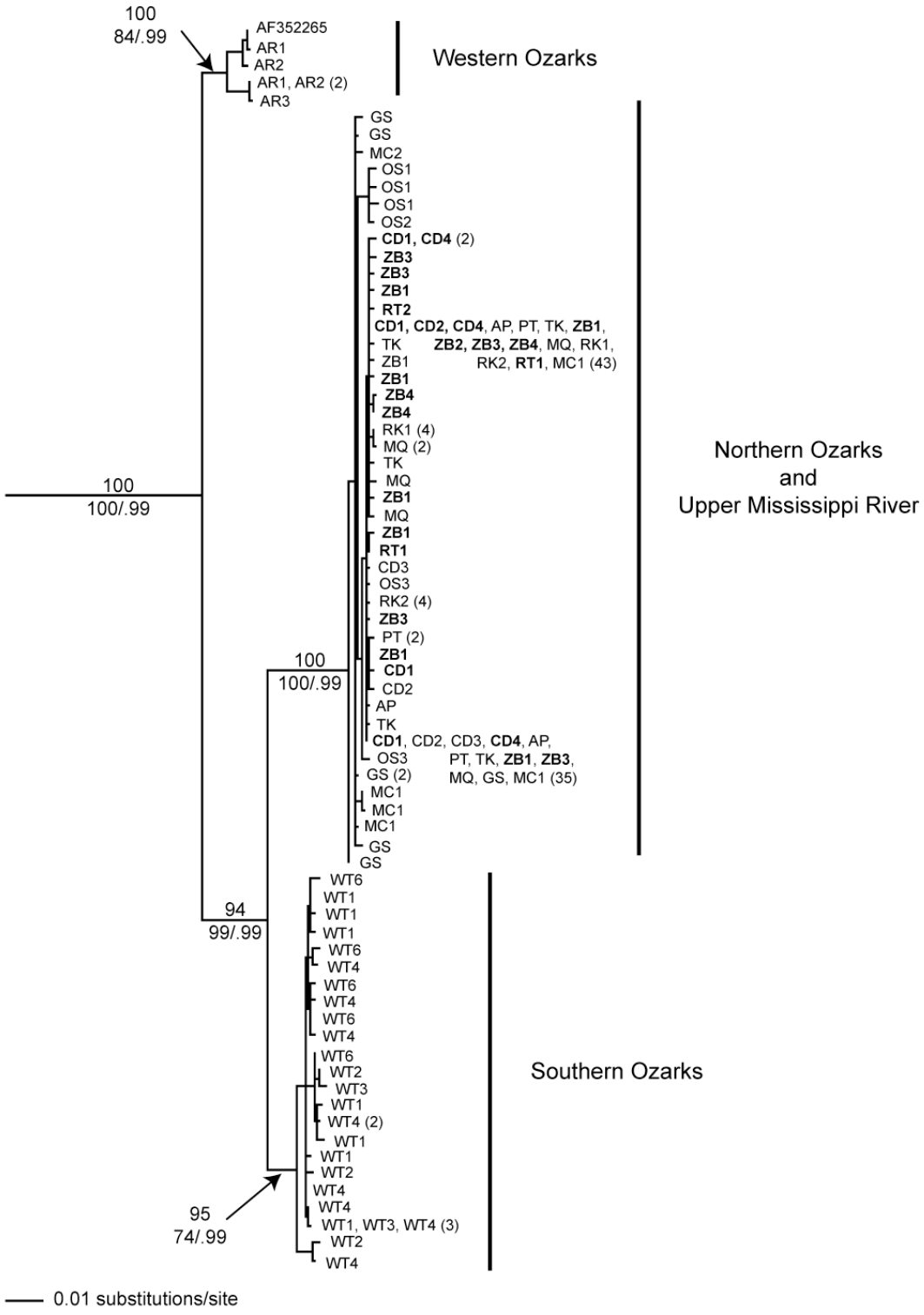

Figure 12. Topology of *Notropis nubilus* haplotypes produced in the maximum likelihood analysis of the cyt*b* data set. Numbers above nodes indicate parsimony bootstrap values. Numbers below nodes indicate maximum likelihood bootstrap values followed by Bayesian posterior probabilities. Outgroups are not shown. Locality ID corresponds to Table 3. Locality IDs in bold are drainages in southeastern Minnesota. Numbers in parentheses indicated number of individuals with identical haplotypes.

Molecular diversity indices of the cyt*b* data set are listed in Table 8. The Western Ozarks contained the greatest amount of nucleotide diversity and the Northern Ozarks and upper Mississippi River contain the least.

Table 11. Molecular diversity of cyt*b* data set for *Notropis nubilus* as determined by the phylogenetic analyses.

Clade	n	Number of Private Haplotypes	Nucleotide Diversity ± SD
Northern Ozarks and upper Mississippi River	127	46	0.0025 ± 0.0015
Southern Ozarks	26	22	0.0058 ± 0.0032
Western Ozarks	7	5	0.0086 ± 0.0052

Of the 79 microsatellite loci screened in *Notropis nubilus* seven were scorable and polymorphic with two or more alleles (Table 12). No significant linkages were found between any pair of loci. There were significant departures from Hardy-Weinberg equilibrium for many of the populations and loci. Due to the large number of alleles, we suggest the scoring of the loci needs to be further examined. However, we continued to analyze these data for any evidence of signal. There were private alleles for each of the groups defined. None of the groups had monomorphic loci. The mean allelic richness was similar across all groups defined; ranging from 6.5051 – 7.924 (Table 12).

Table 12. Summary of microsatellite genetic variation in *Notropis nubilus* including: number of individuals sampled (*n*); number of alleles for each group (*k*); allelic richness (A_R); number of private alleles (N_{PA}); *P* value of exact tests for deviation from expected Hardy-Weinberg equilibrium (HWE); expected (H_E) and observed (H_O) heterozygosities. Asterisk indicates deviation from HWE. Groups are based on the results of phylogenetic and cluster analyses (Figs. 12-14). Specific locality IDs correspond to Table 3.

Locus		Western Ozarks (AR)	Northern Ozarks (GS, OS, MC)	Southern Ozarks (WT)	Upper Mississippi River West (CD, ZB, RT, TK, MQ)	Upper Mississippi River East (RK, PT, AP)
Ppr106	*n*	8	23	35	98	36
(Ardren et al. 2002)	*k*	7	13	15	17	12
Size Range: 152 – 210 bp	A_R	7.000	8.036	8.518	6.180	6.636
Alleles: 21	N_{PA}	0	0	1	2	2
	HWE	0.6569	0.1135	0.6054	0.0867	0.4757
	H_E	6.9333	18.6667	31.5652	72.3782	29.8310
	H_O	1	17	29	63	27
Lco1	*n*	8	23	35	104	36
(Turner et al. 2004)	*k*	10	9	16	10	2
Size Range: 249 – 290 bp	A_R	10.000	5.875	8.822	2.672	2.000
Alleles: 26	N_{PA}	2	1	5	2	0
	HWE	0.1411	*0.0023	*0.000	*0.000	*0.000
	H_E	7.5333	17.1333	31.2174	23.3044	18.0282
	H_O	2	13	21	17	32
Ppro126	*n*	8	25	34	107	36
(Bessert and Orti 2003)	*k*	4	7	9	15	9
Size Range: 173 – 205 bp	A_R	4.000	3.822	5.510	4.919	5.405
Alleles: 20	N_{PA}	0	0	1	5	2
	HWE	0.4860	*0.0000	*0.0001	*0.0000	*0.0003
	H_E	5.8000	15.4694	23.6418	74.2018	27.2958
	H_O	1	23	21	89	29
Ppro132	*n*	8	25	34	106	36
(Bessert and Orti 2003)	*k*	8	25	27	43	28
Size Range: 134 – 165 bp	A_R	8.000	12.232	12.313	12.801	10.772
Alleles: 22	N_{PA}	0	2	5	7	7
	HWE	*0.0000	*0.0000	*0.0000	*0.0000	*0.0000
	H_E	7.2667	24.0205	32.7463	102.6777	33.0281
	H_O	5	18	24	82	26

Table 12 continued…

Locus		Western Ozarks (AR)	Northern Ozarks (GS, OS, MC)	Southern Ozarks (WT)	Upper Mississippi River West (CD, ZB, RT, TK, MQ)	Upper Mississippi River East (RK, PT, AP)
Ca1	*n*	8	25	32	107	36
(Dimsoski et al 2000)	*k*	8	11	16	17	9
Size Range: 100 – 188 bp	A_R	8.000	5.824	8.798	6.207	4.947
Alleles: 59	N_{PA}	1	0	1	2	1
	HWE	*0.0015	*0.0000	*0.0000	*0.0000	*0.0000
	H_E	7.2667	15.7143	27.9841	77.2817	25.6901
	H_O	4	8	22	41	12
Ca6	*n*	8	25	34	105	30
(Dimsoski et al 2000)	*k*	6	9	9	10	16
Size Range: 209 – 231 bp	A_R	6.000	5.161	5.420	3.212	9.292
Alleles: 23	N_{PA}	1	1	1	1	8
	HWE	0.1152	*0.0004	0.3772	*0.0000	*0.0000
	H_E	6.6667	17.3469	24.2239	60.5598	26.3860
	H_O	2	13	21	54	10
Ca16	*n*	8	25	34	105	30
(Dimsoski et al 2000)	*k*	8	8	12	14	12
Size Range: 56 – 204 bp	A_R	8.000	5.148	6.092	6.365	8.205
Alleles: 18	N_{PA}	1	0	3	1	3
	HWE	1.000	*0.0135	*0.0000	*0.0000	*0.0063
	H_E	6.6667	18.1020	25.8358	81.7488	24.0377
	H_O	0	22	34	103	27
Average for all loci	A_R	7.286	6.585	7.924	6.051	6.751
	H_E	6.876	18.078	28.174	70.307	26.317
	H_O	4.286	16.286	24.571	64.143	23.285

Net-between group mean distances for the cyt*b* sequence data and within group distances for both the cyt*b* sequence data and microsatellites are listed in Table 13. These data revealed that there is little diversity within groups for the cyt*b* data, but greater diversity for the microsatellite data. There was greater net between-group divergence for the cyt*b* data than the microsatellite data. in the sequence data and greater diversity in the microsatellites. Population subdivision measured as pairwise F_{ST} was high for the cyt*b* data; however, it was less for the microsatellite data suggesting greater gene flow.

Table 13. On diagonals (in **bold**) are within group average genetic distances [and standard error] for *Notropis nubilus*. Below each diagonal are net between-group mean genetic distances [and standard error] between populations. Above each diagonal are pairwise F_{ST}, based on pairwise distance. All distances estimated using the K2P model. NOUM = Northern Ozarks and upper Mississippi River; WO = Western Ozarks; SO = Southern Ozarks.

Marker	Drainage	NOUM	WO	SO
cyt*b*	NOUM	**0.002 [0.001]**	0.932	0.916
	WO	0.029 [0.006]	**0.009 [0.005]**	0.827
	SO	0.031 [0.005]	0.033 [0.006]	**0.006 [0.003]**
microsatellite	NOUM	**0.694 [0.407]**	0.112	0.116
	WO	---	**0.860 [0.484]**	0.025
	SO	---	---	**0.791 [0.434]**

Across the local populations the AMOVA of the cyt*b* data set revealed that defining groups by regions, upper Mississippi River and Ozarks, explained some of the variation among haplotypes (F_{CT} = 0.43066, $P < 0.001$, Table 14A). However, a lot of the variation was also explained by variation among drainages within the groups (F_{SC} = 0.78878, $P < 0.001$, Table 14A). The AMOVA of the microsatellite data was not consistent with this result; most of the variation was explained within drainages (Table 14C). When the groups were defined by clades identified in the phylogenetic analyses the cyt*b* data revealed most of the variation was explained among clades (Table 14B) where the microsatellite data had more variation within clades (Table 14D).

Table 14. AMOVA variance components for *Notropis nubilus*, percentage variation explained at each spatial level and fixation indices for **A**) cyt*b* data with populations defined by drainage and groups defined by regions of the upper Mississippi River Basin and the Ozarks, **B**) cyt*b* data with clades defined by phylogenetic analyses, **C**) microsatellite data with populations defined by drainage and groups defined by regions of the upper Mississippi River Basin and the Ozarks and **D**) microsatellite data with clades defined by phylogenetc analyses.

A)

Source of variation	d.f	Variance components	Percentage variation	Fixation indices
Among groups	1	4.3738 Va	43.07	F_{CT} = 0.43066 (P<0.001)
Among drainages within groups	11	4.7315 Vb	44.91	F_{SC} = 0.78878 (P<0.001)
Within drainages	147	1.2670 Vc	12.03	
Total	159	10.5360		F_{ST} = 0.87974 (P<0.007)

B)

Source of variation	d.f	Variance components	Percentage variation	Fixation indices
Among clades	2	16.4022 Va	91.02	
Within clades	157	1.6411 Vb	8.98	
Total	159	18.2813		F_{ST} = 0.0926 (P< 0.001)

C)

Source of variation	d.f	Variance components	Percentage variation	Fixation indices
Among groups	2	0.1530 Va	7.82	F_{CT} = 0.0782 (P<0.010)
Among drainages within groups	10	0.1173 Vb	6.00	F_{SC} = 0.0651 (P<0.001)
Within drainages	409	1.6860 Vc	86.18	
Total	421	1.9563		F_{ST} = 0.1382 (P<0.001)

D)

Source of variation	d.f	Variance components	Percentage variation	Fixation indices
Among clades	2	0.2214 Va	11.14	
Within clades	419	1.7657 Vb	88.86	
Total	421	1.9871		F_{ST} = 0.1114 (P< 0.001)

The Bayesian admixture procedure implemented in STRUCTURE (Pritchard et al. 2000) showed a large incremental increase in the likelihood [Pr(*X*/*K*)] as the number of genetic clusters in the model increased from one to four. After four, there continued to be slight increases in the likelihood as the number of clusters used in the model increased to $K = 10$ (Fig. 13). Following the method of Evanno et al. (2005), we determined the distribution of ΔK to have a strong modal value at $K = 2$ and $K = 3$ (Fig. 13). This indicated that the highest level of population structure exists between either two or three genetic clusters. The membership coefficients of each individual in these clusters for $K = 2$ and $K = 3$, along with corresponding localities are shown in Fig. 14. Based on a model assuming two genetically-defined populations ($K = 2$) the majority of individuals from the southern (WT) and western (AR) had over 90% membership in cluster one. There was also high membership of individuals from the upper Mississippi River Basin east of the Mississippi River (RK, AB and PT) in this cluster. The majority of individuals from the northern Ozarks (OS, GS and MC) and the upper Mississippi River Basin west of the Mississippi River (CD, ZB, RT, TK and MQ) had high membership in cluster two. The analysis assuming three genetically-defined populations ($K = 3$) again clustered individuals from the southern (WT) and western (AR) Ozarks; cluster one. However, the majority of individuals from the upper Mississippi River Basin east of the Mississippi River (RK, AP and PT) had high membership in cluster two and where distinct from the southern and western Ozarks. Several individuals from the Zumbro River (ZB) west of the Mississippi also clustered with individuals east of the Mississippi River. Most individuals from the northern Ozarks and the upper Mississippi River west of the Mississippi River grouped into a third cluster. However, there were some individuals with membership in clusters one and two.

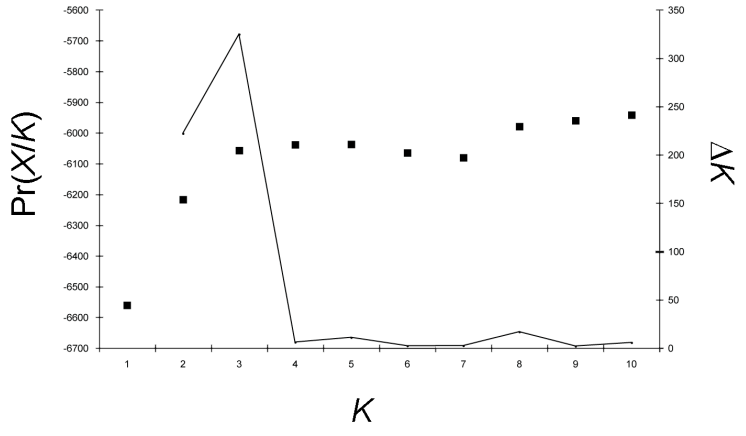

Figure 13. Plot of the number of genetically discrete populations (*K*) in *Notropis nubilus* versus the two optimality criteria: the raw average -Ln likelihood indicated by the squares and scaled to the left vertical axis (Pritchard et al. 2000) and ΔK (Evanno et al. 2005) indicated by the solid line and scaled to the right vertical axis.

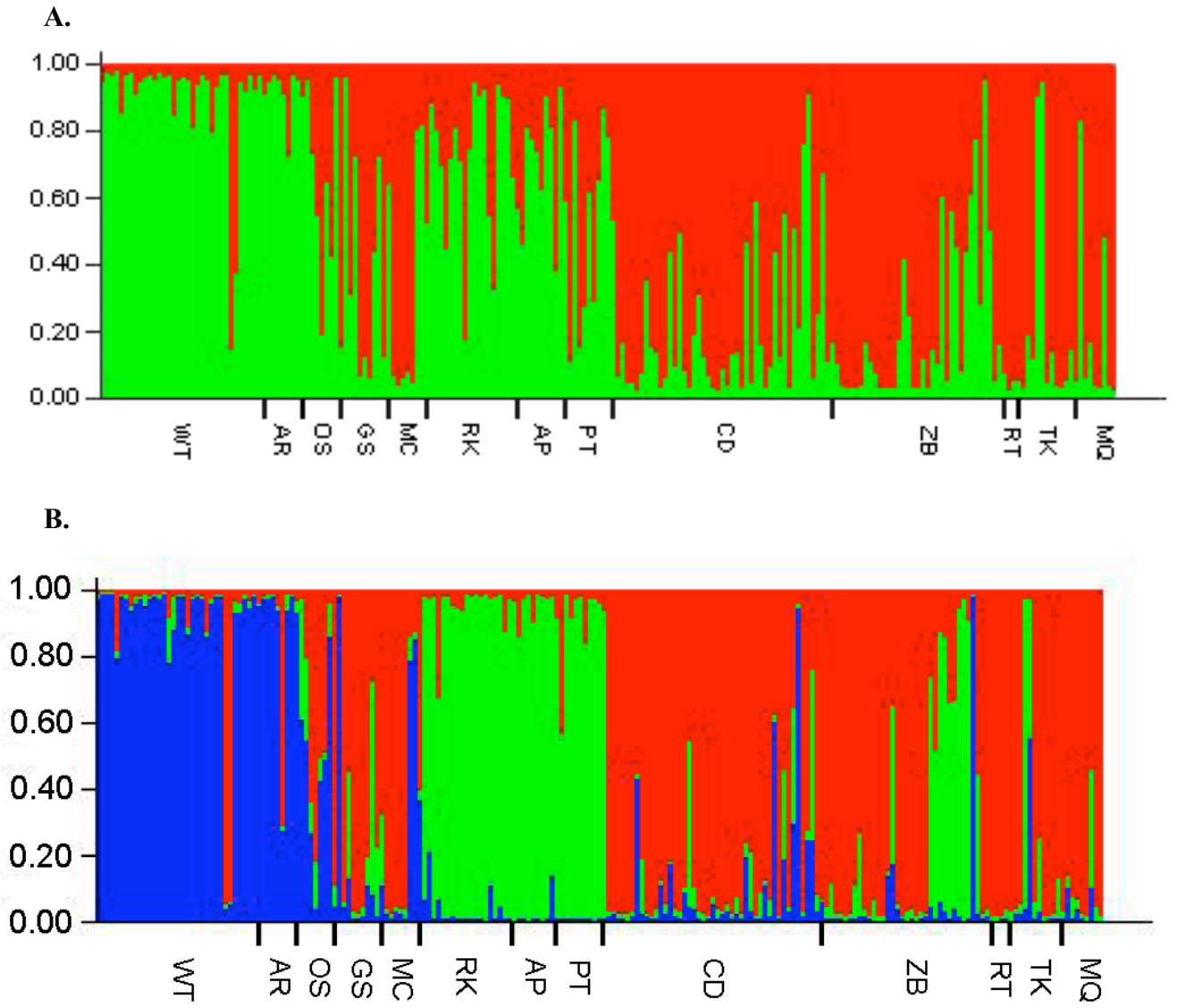

Figure 14. Estimated membership coefficients in *Notropis nubilus* based on admixture analyses for (**A**) $K = 2$ and (**B**) $K = 3$ genetically defined populations for each individual sampled. Vertical axis indicates membership coefficient and the horizontal axis indicates the population of each individual. Locality IDs correspond to Table 3.

DISCUSSION

Southeastern Minnesota is a distinct geographic region within Minnesota that contains a large amount of diversity that is unique to the state. *Clinostomus elongatus*, *Lythrurus umbratilis* and *Notropis nubilus* are three fishes that are distributed in this region that have been recognized as in need of conservation in Minnesota's Comprehensive Wildlife Conservation Strategy. The occurrence of these fishes in southeastern Minnesota is likely the result of relict populations that survived the last glacial episode. The results of this study revealed different patterns and scales of genetic variation for each species within southeastern Minnesota. Therefore, recommendations for the establishment of a framework for maintenance of genetic diversity are given individually for each species.

Within *Clinostomus elongatus* there is very little cyt*b* variation; however, the microsatellite data revealed significant genetic differentiation by drainage. The phylogenetic analyses of the cyt*b* data in the redside dace lacked resolution; there was a single clade containing all haploytpes including individuals from the Zumbro, Cannon and Root rivers and Ohio (Fig. 8). The genetic divergences were also very low (Table 6). Based on these data there was no evidence of independent genetic units in southeastern Minnesota. The microsatellite data uncovered finer scale diversity within the group. Results of the F_{ST} (Table 6) and Bayesian assignment test (Fig. 10) of the microsatellite data showed evidence of genetic uniqueness. Each drainage in southeastern Minnesota and Ohio was genetically distinct (Fig. 10). Although the results of the AMOVA analyses of the microsatellite data did reveal that there was also a significant amount of variation within each drainage (Table 7). Based on the microsatellite data in *C. elongatus* genetic units can be defined by drainage. Therefore, we recommend that conservation efforts directed towards maintaining the genetic diversity of this species focus on each drainage, Zumbro, Cannon and Root rivers, separately.

Lythrurus umbratilis exhibits widespread cyt*b* variation across the range of the species. The phylogenetic analyses of the cyt*b* data in the redfin shiner recovered three strongly supported clades (Fig.11). These clades are largely consistent with geography; however, each clade also contained individuals from outside the general region of the remainder haplotypes within the clade. Most of the individuals from drainages within southeastern Minnesota were contained within a single clade (Fig. 11). However, this clade also contained individuals from the St. Francis River in the southern Ozarks that had an identical haplotype with an individual from the Cedar River. In addition, haplotypes from the upper Mississippi River basin were also included in clades that predominantly contained haplotypes from the northern and southern Ozarks. The genetic divergence between these clades was high, ranging from 0.24 – 0.70 (Table 9). The results of the analyses suggest that this is a widespread

population and there is no evidence of genetic distinctiveness within southeastern Minnesota. Therefore we recommend that conservation efforts directed towards maintaining the genetic diversity within this species treat all populations as a single genetic unit and focus collectively on all of their native drainages in the state: Zumbro, Root, Upper Iowa and Cedar rivers.

Within *Notropis nubilus* there are regional differences in the cyt*b* and microsatellite variation. The phylogenetic analyses of the cyt*b* data in the Ozark minnow recovered three strongly supported clades, which exhibited unique sets of haplotypes consistent with geographic distributions (Fig.12). There was deep divergence among haplotypes from the Ozarks. Haplotypes from the western Ozarks formed a monophyletic group that was sister to a clade containing haplotypes from the southern Ozarks and a clade containing haplotypes from the northern Ozarks plus upper Mississippi River Basin. Based on these results we suggest that there may be greater species diversity within the group. Individuals from drainages in southeastern Minnesota were included in the clade containing the northern Ozarks and upper Mississippi River Basin. Within this clade there were short branch lengths and no geographic structuring. The pattern of a close relationship between the northern Ozarks and upper Mississippi River is a pattern observed in other clades of fishes (Near et al. 2001; Berendzen et al. 2003; Berendzen et al. 2008). Based on these data there was no evidence of independent genetic units in southeastern Minnesota. The microsatellite data uncovered finer scale diversity within the group in the upper Mississippi River Basin. Results of the Bayesian assignment test (Fig. 14) of the microsatellite data showed evidence of genetic structure. This analyses revealed a genetic distinction between individuals in drainages east and west of the Mississippi River in the upper Mississippi River Basin. This suggests that the Mississippi River is a barrier to gene flow. However, there was also some indication of genetic relatedness between individuals from the Zumbro River and populations east of the Mississippi River (Fig. 14). These data need to be further explored to estimate the amount and direction of gene flow. Based on the cyt*b* data genetic units can be defined in the western Ozarks, southern Ozarks and northern Ozarks plus upper Mississippi River Basin. Based on the microsatellite data in *Notropis nubilus* genetic units can be defined by drainages east and west of the Mississippi River. Therefore we recommend that conservation efforts directed towards maintaining the genetic diversity within this species treat all populations as a single genetic unit and focus collectively on all of their native drainages in the state: Zumbro, Root and Cedar rivers.

A single population of *Noturus exilis* (slender madtom) occurs in Minnesota and specimens were unable to be collected. Therefore, *Noturus exilis* was not included in this project.

ACKNOWLEDGMENTS

We thank Konrad Schmidt, Nongame Fish Specialist, Division of Ecological Services Minnesota Department of Natural Resources, for acting as the DNR liaison on this grant, providing locality information and assisting in the collection of samples. We also thank Andrew Simons (Curator of Fishes), Jacob Egge and Brett Nagle at the Bell Museum of Natural History, University of Minnesota for providing locality data and tissue samples, and depositing voucher material. We thank John Lyons, Wisconsin Department of Natural Resources, for valuable discussion on these fishes. Finally, we thank Scott Barron, Katie Berge, Alex DeWitt, Larry Hilton, Dana Hubbard, Derek Stewart, Jeff Tamplin and Alexa Warwick for help with collecting specimens and laboratory work.

LITERATURE CITED

Ardren, W. R., Miller, L. M. Kime, J. A. and Kvitrud, M. A. (2002) Microsatellite loci for fathead minnow (*Pimephales promelas*). *Molecular Ecology*. 2002(2):226-227.

Becker, G. C. (1983) Fishes of Wisconsin. Madison, Wisconsin, The University of Wisconsin Press.

Berendzen, P. B., Simons, A. M. and Wood, R. M. (2003) Phylogeography of the northern hogsucker, *Hypentelium nigricans* (Teleostei: Cypriniformes): genetic evidence for the existence of the ancient Teays River. *Journal of Biogeography*. 30:1139-1152.

Berendzen, P. B., Simons, A. M., Wood, R. M., Dowling, T. E. and Secor C. L. (2008) Recovering cryptic diversity and ancient drainage patterns in eastern North America: Historical biogeography of the *Notropis rubellus* species group (Teleostei: Cypriniformes). *Molecular Phylogenetics and Evolution*. 46(2):721-737.

Bessert, M. L. and Orti, G. (2003) Microsatellite loci for paternity analysis in the fathead minnow, *Pimephales promelas* (Teleosti: Cyprinidae). *Molecular Ecology*. 2003(3):532-534.

Bielawski, J. P. and Gold, J. R. (2001) Phylogenetic relationships of Cyprinid fishes in subgenus *Notropis* inferred from nucleotide sequences of mitochondrially encoded cytochrome *b* gene. *Copeia*. 2001(3):656-667.

Boutin-Ganache, I., Raposo, M., Raymond, M. and Deschepper, C. F. (2001) M13-tailed primers improve the readability and usability of microsatellite analyses performed with two different allele-sizing methods. *Biotechniques*. 31:25-28.

Burr, B. M. and Page, L. M. (1986) Zoogeography of fishes of the Lower Ohio-Upper Mississippi basin. *The Zoogeography of North American Fishes* (ed. by C. H. Hocutt and E. O. Wiley), pp. 287-324. New York: Wiley Interscience.

Canadian Redside Dace Recovery Team 2005. Redside Dace Recovery Strategy. http://www.elgar.ca/creekbank/New%20Redside%20Dace%20Recovery%20Strategy%20-%20January%2031%202005.pdf

Culter, P., Mickleson, D., Colgan, P. MacAyeal, D. and Parizek, B. (2001) Influence of the Great Lakes on the dynamics of the southern Laurentide ice sheet: numerical experiments. *Geology*. 29:1039-1042.

Demastes, J. W., Eastman, J. M., East, J. S. and Spolsky, C. (2007) Phylogeopgraphy of the Blue-spotted slalmander, *Ambystoma laterale* (Caudata: Ambysomatidae). *American Midland Naturalist*. 157:149-161.

Dimsoski, P., Toth, G. P. and Bagley, M. J. (2000) Microsatellite characterization in central stoneroller *Campostoma anomalum* (Pisces: Cyprinidae). *Molecular Ecology*. 2000(9):2155-2234.

Edwards, S. V. (1997) Relevance of microevolutionary processes to higher level molecular systematics. *Avian Molecular Evolution and Systematics* (ed. by D.P. Mindell). 251-278. Academic Press, San Diego.

El Mousadik, A. and Petit, R. J. (1996) High level of genetic differentiation for allelic richness among populations of the argan tree [*Argania spinosa* (L.) Skeels] endemic to Morocco. *Theoretical Applied Genetics*. 92:832-839.

Evanno, G., Regnaut, S. and Goudet, J. (2005) Detecting the number of clusters of individuals using the software STRUCTURE: a simulation study. *Molecular Ecology*. 14(8):2611-2620.

Excoffier, L., Laval, G. and Schneider, S. (2005) Arlequin ver. 3.0: An integrated software package for population genetics data analysis. *Evolutionary Bioinformatics Online.* 1:47-50.

Excoffier, L., Smouse, P. E. and Quattro J. M. (1992) Analysis of molecular variance inferred from metric distances among DNA haplotypes, application to human mitochondrial DNA restriction data. *Genetics*. 131:479-491.

Felley, J. D. and Hill, L. G. (1983) Multivariate assessment of environmental preferences of cyprinid fishes of the Illinois river, Oklahoma. *American Midland Naturalist*. 109(2):209-221.

Felsenstein, J. (1985) Confidence limits on phylogenies: an approach using the bootstrap. *Evolution*. 39:783-791.

Fowler, J. F., James, P. W. and Taber, C. A. (1984) Spawning activity and eggs of the Ozark minnow, *Notropis nubilus*. *Copeia*. 1984(4):994-996.

Girard, P. and Angers, B. (2006) Characterization of microsatellite loci in longnose dace (*Rhinichthys cataractae*) and interspecific amplification in five other Leuciscinae species. *Molecular Ecology*. 2006(6):69-71.

Glazier, J. R. and Taber, C. A. (1980) Reproductive biology and age and growth of the Ozark minnow, *Dionda nubile*. *Copeia*. 1980(3):547-550.

Goudet, J. (1995) FSTAT (Version 1.2): a computer program to calculate F-statistics. *Journal of Heredity*. 86:485-486.

Hobbs, H. (1999) Origin of the driftless area by subglacial drainage-a new hypothesis. *Geological Society of America*. Special Paper 337:93-102.

Huelsenbeck, J. P. and Ronquist, F. R. (2001) MRBAYES: Bayesian inference of phylogeny. *Bioinformatics.* 17:154-755.

Iqbal, M. Z. (1998) Application of environmental isotopes in storm-discharge analysis of two contrasting stream channels in a watershed. *Water Research*. 32(10):2959-2968.

Koster, W. (1939) Some phases of the life history and relationships of the cyprinid, *Clinostomus elongatus* (Kirtland). *Copeia*. 1939:201–208.

Kumar, S., Tamura, K. and Nei, M. (2004) MEGA3: integrated software for molecular evolutionary genetics analysis and sequence alignment. *Briefings in Bioinformatics*. 5:150-163.

Lee, D. S., Gilbert, C. R., Hocutt, C. H., Jenkins, R. E., McAllister, D. E. and Staugger, J. R. Jr. (1980) Atlas of North American Freshwater Fishes. N. C. State Museum of Natural History. Raleigh, North Carolina. 854p.

Matthews, M. M. and Heins, D. C. (1984) Life History of the Redfin Shiner, *Notropis umbratilis* (Pisces: Cyprinidae), in Mississippi. *Copeia.* 1984(2):385-390.

Mayden, R. L. (1988) Vicariance biogeography, parsimony, and evolution in North American freshwater fishes. *Systematic Zoology*. 37:329-355.

NatureServe. (2007) NatureServe Explorer: An online encyclopedia of life [web application]. Version 6.2. NatureServe, Arlington, Virginia. Available http://www.natureserve.org/explorer. (Accessed: January 23, 2008).

Near, J. T., Page, L. M. and Mayden, R. L. (2001) Intraspecific phylogeography of *Percina evides* (Percidae: Etheostomatinae): an additional test of the central highlands pre-Pleistocene vicariance hypothesis. *Molecular Ecology*. 10:2235-2240.

Nei, M. and Li, W. (1979) Mathematical model for studying genetic variation in terms of restriction endonucleases. *Proceedings of the National Academy of Sciences USA*. 76:5269-5273.

Novinger, D. C. and Coon, T. G. (2000) Behavior and physiology of the redside dace, *Clinostomus elongatus*, a threatened species in Michigan. *Environmental Biology of Fishes*. 57:315-326.

Nylander, J. A. A. (2004) MrModeltest v2. Program distributed by the author. Evolutionary Biology Centre, Uppsala University.

Page, L. M. and Burr, B. M. (1991) A field guide to freshwater fishes, North America north of Mexico. Houghton Mifflin, Boston, Massachusetts.

Pflieger, W. L. (1975) The Fishes of Missouri. Missouri Department of Conservation.

Posada, D. and Buckley, T. R. (2004) Model selection and model averaging in phylogenetics: advantages of Akaike information criterion and Bayesian approaches over likelihood ratio tests. *Systematic Biology*. 53:793-808.

Posada, D. and Crandall, K. A. (1998) Modeltest: Testing the model of DNA substitution. *Bioinformatics*. 14:817-818.

Pramuk, J. B., Grose, M. J., Clark, A. L., Greenbaum, E., Bonaccorso, E., Guayasamin, J. M., Smith-Pardo, A. H., Benz, B. W., Harris, B. R., Siegfreid, E., Reid, Y. R., Holcroft-Benson, N. and Wiley, E. O. (2007) Phylogeny of finescale shiners of the genus *Lythrurus* (Cypriniformes: Cyprinidae) inferred from four mitochondrial genes. *Molecular Phylogenetics and Evolution*. 42(2007):287-297.

Pritchard, J. K., Stephens, M. and Donnely, P. (2000) Inference of population structure using multilocus genotype data. *Genetics*. 155:945-959.

Raymond, M. and Rousset, F. (1995) GENEPOP (Web version, 2005). Population genetics software for exact tests and ecumenicism. *Journal of Heredity*. 86:248-249.

Ronquist, F. R. and Huelsenbeck, J. P. (2003) MrBayes 3: Bayesian phylogenetic inference under mixed models. *Bioinformatics*. 19:1572-1574.

Ruhe R. V., Dietz W. P., Fenton, T. E. and Hall G. F. (1968) Iowan drift problem, north-eastern Iowa. *Iowa Geological Survey Report of Investigations*, No. 7, 40 p.

Schmidt, T. R., Biewalski, J. P. and Gold, J. R. (1998) Molecular phylogenetics and evolution of the cytochrome *b* gene in the cyprinid genus *Lythrurus* (Actinopterygii: Cypriniformes). *Copeia*. 1998:14-22.

Schuelke, M. (2000) An economic method for the fluorescent labeling of PCR fragments. *Nature biotechnology*. 18:233-234.

Simons, A. M., Berendzen, P. B. and Mayden, R. L. (2003) Molecular systematics of North American phoxinin genera (Actinopterygii: Cyprinidae) inferred from mitochondrial 12S and 16S ribosomal RNA sequences. *Zoological Journal of the Linnean Society*. 139:63-80.

Skalski, G. T. and Grose, M. J. (2006) Characterization of microsatellite loci in the creek chub (*Semotilus atromaculatus*). *Molecular Ecology Notes.* 6(4):1240-1242.

Snelson, F. F., and Pflieger, W. L. (1975) Redescription of the Redfin Shiner, *Notropis umbratilis*, and Its Subspecies in the Central Mississippi River Basin. *Copeia.* 1975(2):231-249.

Swofford, D. L. (2001) PAUP*: Phylogenetic analysis using parsimony, version 4.0b10. Sunderland, MA. Sinauer Associates.

Turner, T. F., Dowling, T. E., Broughton, R. E. and Gold, J. R. (2004) Variable microsatellite markers amplify across divergent lineages of cyprinid fishes (subfamily Leuscinae). *Conservation Genetics*. 5:279-281.

Zwickl, D. J. (2006) Genetic algorithm approaches for the phylogenetic analysis of large biological sequence datasets under the maximum likelihood criterion. Ph.D. dissertation, The University of Texas at Austin.